Miscellaneous Paper W-94-1
December 1994

US Army Corps of Engineers
Waterways Experiment Station

Water Operations Technical Support Program

Oxygen Transfer Similitude for a Vented Hydroturbine

by Eric J. Thompson, University of Minnesota

Approved For Public Release; Distribution Is Unlimited

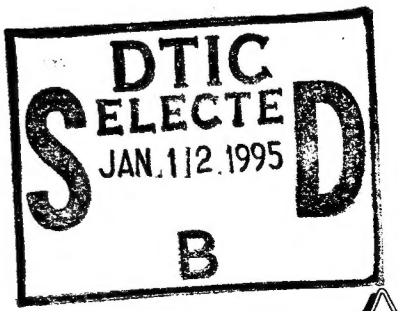

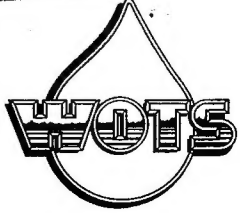

Prepared for Headquarters, U.S. Army Corps of Engineers

Water Operations Technical Support Program

Miscellaneous Paper W-94-1
December 1994

Oxygen Transfer Similitude for a Vented Hydroturbine

by Eric J. Thompson

St. Anthony Falls Hydraulic Laboratory
Department of Civil and Mineral Engineering
University of Minnesota
Minneapolis, MN 55414

Final report

Approved for public release; distribution is unlimited

Prepared for U.S. Army Corps of Engineers
Washington, DC 20314-1000

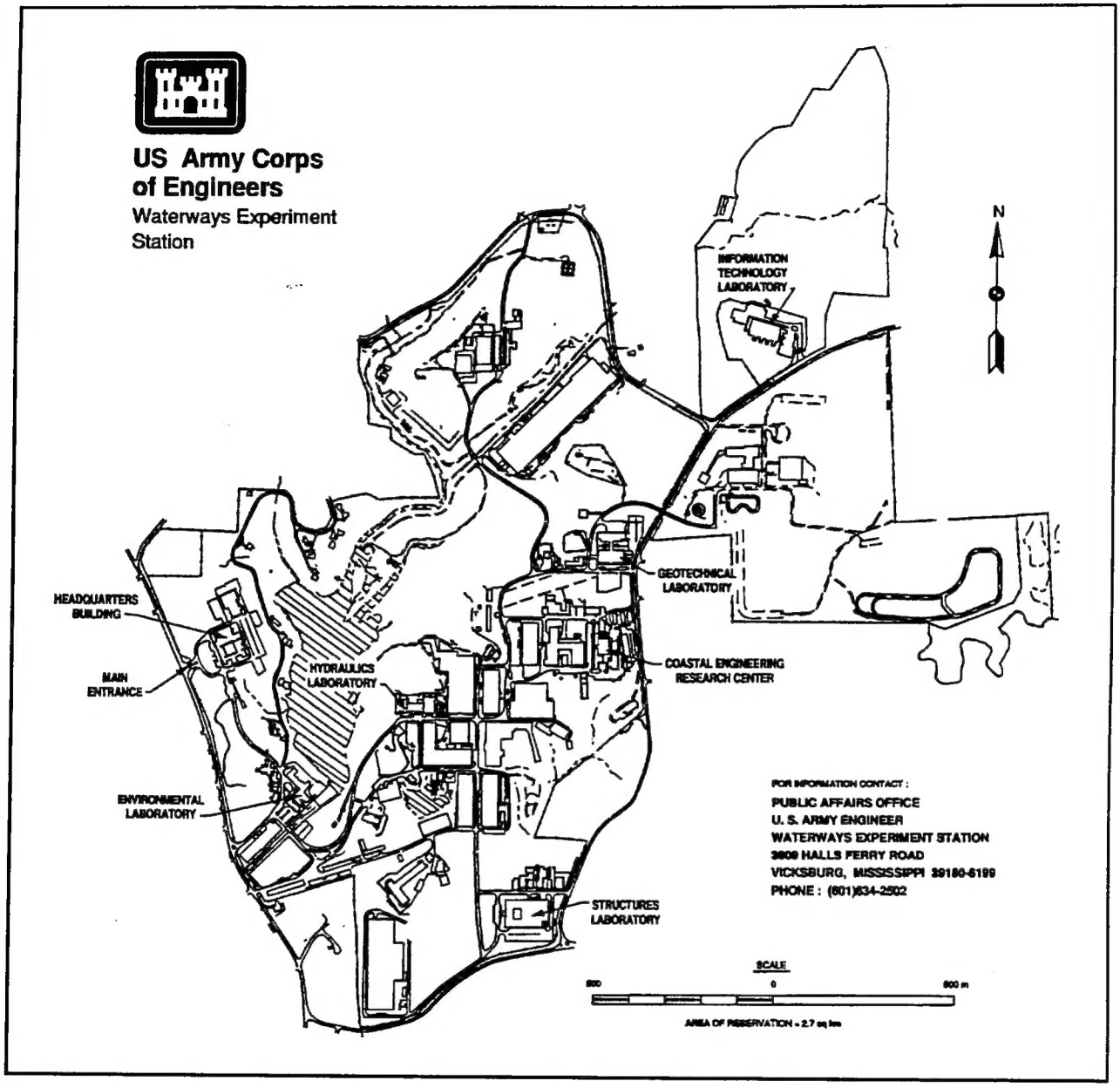

Waterways Experiment Station Cataloging-in-Publication Data

Thompson, Eric J.
Oxygen transfer similitude for a vented hydroturbine / by Eric J. Thompson ; prepared for U.S. Army Corps of Engineers.
83 p. : ill. ; 28 cm. — (Miscellaneous paper ; W-94-1)
Includes bibliographic references.
1. Water — Dissolved Oxygen — Measurement. 2. Turbomachines — Fluid dynamics. 3. Engineering models — Mathematics. 4. Water — Aeration — Evaluation. I. United States. Army. Corps of Engineers. II. U.S. Army Engineer Waterways Experiment Station. III. Water Operations Technical Support Program. IV. Title. V. Series: Miscellaneous paper (U.S. Army Engineer Waterways Experiment Station) ; W-94-1.
TA7 W34m no.W-94-1

Contents

List of Figures

List of Tables

Preface

The work reported herein was funded, in part, by the Water Operations Technical Support (WOTS) Program. The WOTS program is sponsored by the Headquarters, U.S. Army Corps of Engineers (HQUSACE), and is assigned to the U.S. Army Engineer Waterways Experiment Station (WES) under the purview of the Environmental Laboratory. The WOTS Program is managed under the Environmental Resources Research and Assistance Programs (ERRAP), Mr. J. L. Decell, Manager. Mr. Robert C. Gunkel was Assistant Manager, ERRAP, for WOTS. Technical Monitors during this study were Messrs. Frederick B. Juhle and Rixie Hardy, HQUSACE.

This report details an investigation into the development of modeling criteria for oxygen uptake in model and full-scale hydraulic turbines. The research was conducted by the St. Anthony Falls Hydraulic Laboratory (SAFHL) of the Department of Civil and Mineral Engineering, University of Minnesota, under contract with the Reservoir Water Quality Branch, Hydraulics Laboratory (HL), WES. Mr. Steven C. Wilhelms, RWQB, was the WES point of contact. The work was conducted under the general direction of Messrs. Frank A. Herrmann, Jr., Director, HL, and Glenn A. Pickering, Chief, Hydraulic Structures Division, HL.

This report was prepared by Mr. Eric J. Thompson of the SAFHL in partial fulfillment of the requirements for the degree of Master of Science from the University of Minnesota. Dr. John Gulliver, SAFHL, was Mr. Thompson's Faculty Advisor.

At the time of publication of this report, Director of WES was Dr. Robert W. Whalin. Commander was COL Bruce K. Howard, EN. Dr. Roger L. A. Arndt was Director, SAFHL.

This report should be cited as follows:

> Thompson, E. J. (1994). "Oxygen Transfer Similitude for a Vented Hydroturbine," Miscellaneous Paper W-94-1, U.S. Army Engineer Waterways Experiment Station, Vicksburg, MS 39180-6199.

Acknowledgements

This paper is based upon research supported by the Reservoir Water Quality Branch of the U.S. Army Engineer Waterways Experiment Station and by the Minnesota State Legislature ML. 89, Chapt. 335, Art. 2, Sec. 1, Subd. 6 as recommended by the Legislative Commission on Minnesota Resources.

I would, of course, like to thank my advisor, Dr. John S. Gulliver who was readily available for questions and who guided my research from beginning to end.

I would like to thank Paul Hopping, Mark Mobley, and Tom Brice of the Tennessee Valley Authority for sharing their AVT data with me. I would also like to thank Steven Wilhelms for his continuing encouragement and support as well as allowing me an opportunity to work in the field in an interesting vented turbine study.

Conversion Factors, Non-SI to SI Units of Measurement

Non-SI units of measurement used in this report can be converted to SI units as follows:

Multiply	By	To Obtain
feet	0.3048	meters
gallons	3.785412	cubic decimeters
inches	2.54	centimeters
cubic feet	0.02831685	cubic meters

I. Introduction

Currently there is much emphasis placed upon water quality and maintaining water quality parameters in our freshwater hydrosphere. One of the most widely cited parameters is that of dissolved oxygen concentration (DO). DO is often used as an indicator of the quality of water for use by humans as well as habitat for aquatic flora and fauna, and is maintained by many natural chemical and biochemical processes which either increase or decrease local oxygen concentrations. Respiration by aquatic life serves to reduce DO, as does biodegradation of organic material in the sediments, along with a host of other oxygen consuming chemical reactions. Photosynthesis by aquatic plant life can be a significant source of oxygen to a water body, as can oxygen mass transfer with the atmosphere. In nature these processes result in balanced DO concentrations, allowing for seasonal changes, in surface waters.

Large impoundments of water, such as those found behind hydropower facilities, upset this delicate balance and can have severe effects on water quality. As illustrated by Figure 1.1, spillways withdraw well-mixed surface waters from reservoirs where DO concentrations are high, and toxins, metals, and high nutrient concentrations (symptoms of low DO) are low. Spillways are also very effective aerators, enhancing DO levels by exposing large surfaces of turbulent water to the atmosphere, thus restoring the environment (in terms of oxygen transfer) for the river reach that was made into a slow moving reservoir.

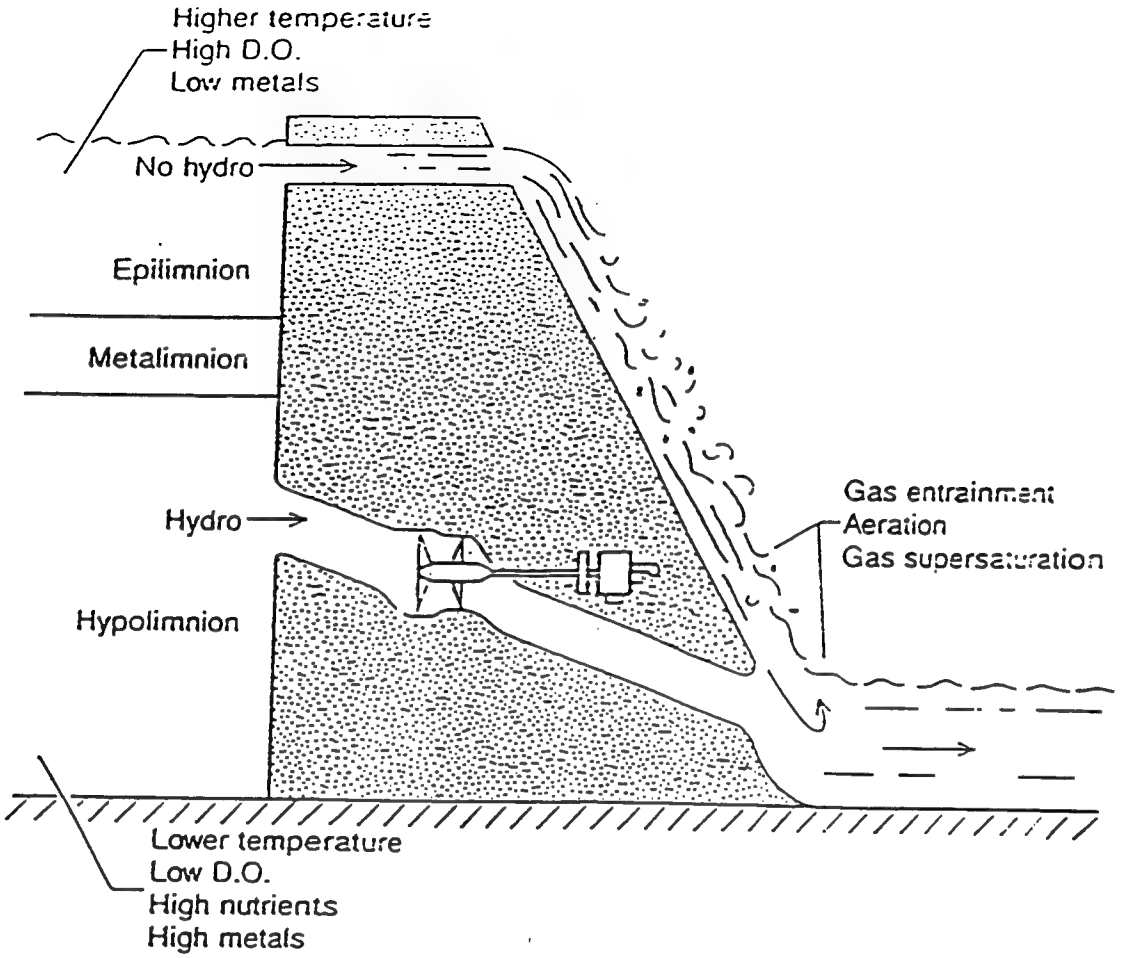

Figure 1.1 Water quality changes due to hydropower operation at dams
(Arndt and Gulliver, 1989)

Turbine intakes, however frequently release water from the hypolimnion of reservoirs; where, due to thermal (density) stratification, DO concentrations are often quite low. Thermal stratification occurs in the summer months as solar radiation is absorbed as heat by surface waters, causing density differences in reservoir depth profiles. Typically a reservoir will separate into two distinct levels, the epilimnion, a surface layer of warm, less dense water, and the hypolimnion, a deeper level of relatively cool water, with some intermediate levels collectively called the metalimnion. Because of continued exposure to the atmosphere, and relatively high levels of photosynthesis, DO concentrations in the epilimnion are often near saturation (Cole, 1983). However, because of density stratification between the separate levels and the corresponding reduction in turbulent transport, oxygen transfer to lower reservoir levels may be limited. In areas where hypolimnetic oxygen demand exceeds oxygen replenishment, as is the case in many hydropower reservoirs, DO levels may drop to anoxic (zero DO) conditions.

The concerns for low DO associated with hydroelectric installations primarily involve the preservation of aquatic habitat. Under anoxic conditions, several problems may develop which endanger the lives of fish and other aquatic lifeforms; trace metals and nutrients may be released from sediments, high concentrations of hydrogen sulfide may result from anaerobic biodegradation, and the pH of the water body may drop (Wilhelms, 1987). Dissolved oxygen concentrations approaching zero will create extensive mortality of fish and other components of the aquatic biota. The

impacts of poor quality water discharges can extend for tens of river miles downstream of hydroelectric reservoirs. For this reason there is significant interest in alleviating the downstream impacts of these hydroelectric releases.

To reduce or eliminate the problems associated with low DO, the U.S. Army Corps of Engineers (USACE), the Tennessee Valley Authority (TVA), the Alabama Power Company (APC), the U.S. Bureau of Reclamation, and others (March et al, 1992) have been researching various means of increasing DO concentration in hydroelectric tailwaters. One of the most attractive techniques currently being investigated is the auto-venting turbine (AVT).

An auto-venting turbine is a hydroturbine that has pressure relieving ports which are open to the atmosphere. When operating at low flows, strong negative pressures which may be damaging to the turbine are relieved by allowing air to enter the turbine draft tube. Because it is not necessary to inject the air using pumps or compressors, turbines which operate this way are said to be auto-venting (Waldrop, 1992).

In most Francis and Kaplan style turbines there exists an apparatus called a vacuum-breaker assembly which allows air to enter the turbine draft tube, usually at the runner nose cone, for purposes of relieving strong negative pressures which can lead to cavitation and draft tube surging. A side effect of this air venting is that a

substantial amount of mass transfer occurs between the water in the draft tube and the oxygen in the air. Tests performed at several hydropower facilities by the Tennessee Valley Authority and the Alabama Power Company have shown that tailwater dissolved oxygen levels may be increased by as much as 2 mg/l over that of the reservoir headwater by atmospheric venting through the vacuum-breaker valve (Wilhelms et al, 1987).

In areas where hydroelectric discharges have depressed levels of dissolved oxygen, facilities may be operated under conditions where the turbines naturally aspirate tailwaters to improve downstream DO. Unfortunately, because most vacuum-breaker systems use automatic cam-operated valves which are only open at lower gate settings, venting occurs only at low discharges (Bohac & Ruane, 1990). Furthermore, adding air tends to reduce the water flow through turbines, resulting in losses in power production and in some cases reduction in operating efficiencies. As a result, AVT research has focused on improving the airflow and oxygen transfer through vented hydroturbines while retaining operating performance.

Since many of the hydropower projects which are operated in the United states are nearing the end of their useful lifetimes, and many newer hydroelectric projects need to be relicensed by the year 2000 (Bohac & Ruane, 1992) recent efforts have gone beyond testing simple alterations on existing Francis runners.

TVA has initiated a research program including the construction of several model and full-scale turbine runners which allow for variations in design that retrofit turbine runners simply could not provide. Previous tests had been performed on full-scale Francis runners modified by adding vents and baffles. The aeration performance of these retrofit turbines suggested that a newly designed auto-venting turbine runner may result in greatly improved aeration efficiencies.

The process of hydroturbine runner creation involves a theoretical design with consideration given to initial performance guidelines. In a relatively new field, such as vented oxygen transfer, new runner development typically incorporates a scale model. Performance testing on the turbine model can be used to provide insight into the full-scale turbine runner. While turbine similitude, the scaling of hydraulic test results between geometrically similar turbines of different sizes, is an old and relatively standardized process, current similitude theory does not provide for mass transfer and the scaling of this phenomenon between models and full-sized installations. As a result it is difficult to predict the oxygen transfer performance of field scale installations from model operational data.

One component of the research comprising the AVT project has been the development of scaling criteria for the auto-venting turbine under various venting configurations. It is the purpose of this thesis to develop a similitude relationship for the gas transfer that occurs in an auto-venting turbine with specific reference to

scaling between a homologous turbine model and a full-size installation, regardless of the turbine operating conditions. The relation is developed with existing theories of air-water mass transfer, bubble hydrodynamics, and turbine hydrodynamics. Data from TVA's Norris model and the full-scale installation, the only model/full-scale data set currently available, will be used to empirically fit and test the similitude theory.

II. History of Auto-Venting Turbine Research

In the United States, the use of hydroturbines for river aeration began in Wisconsin around 1945 to mitigate the effects of paper industry effluents and municipal sewage waters. Aspiration was generally accomplished by simple draft tube venting but in some cases was done through specially designed concrete foundations. Because of serious efficiency losses, aspiration was typically only performed when DO levels dropped below 3 ppm (Bohac et al, 1983).

With impending water quality legislation requiring minimum DO levels in hydropower releases, aeration studies began across the country with many organizations involved in hydropower operation conducting experiments on various installations. Duke Power Company, in 1965, used turbine aeration at its Wylie Station Dam in South Carolina in experiments to reaerate the Catawba river which received high biochemical oxygen demand (BOD) loads from textile plants and paper mills. While there were no power loss measurements performed, DO uptakes were measured at 2.9 ppm. Among others, Portland General Electric Company, in Oregon was examining Willamette Falls along the Willamette river (Amberg et al, 1969), the U.S. Army Corps of Engineers was testing Table Rock Dam in Missouri (Weithman et al, 1980) and Clarks Hill Dam in Georgia and South Carolina (Maudlin, 1982), and the Idaho Power company was performing experiments at American Falls Dam in Idaho (Bohac et el, 1983).

In an effort to increase aeration efficiency, D. C. Raney, working at the University of Alabama in a project sponsored by the Alabama Power Company, developed defector plates which, when placed upstream of air injection ports, cause local reductions in draft tube pressures (Raney & Arnold, 1973; Raney, 1977). These pressure reductions aspirated greater quantities of air and resulted in more oxygen transfer at higher water flow rates. An illustration of a typical auto-venting turbine is given in figure 2.1.

Later that decade, TVA began to improve upon the deflector plates to provide more aeration capacity and reduce the power generation efficiency losses associated with their use. A significant development was 'streamlined baffles' for use on Francis turbine runner nose cones. Then, in 1979, TVA began venting studies at three dams in the Tennessee river system. Norris, Douglas, and Cherokee dams were the sites chosen for a series of tests including air venting through modification of turbine vent-valves and installation of baffle rings near the top of the draft tubes as well as on the turbine runner hub (nose cone). The tests indicated a loss of approximately 3% in turbine efficiency when the deflector plates were used to aspirate air at a relative air volume of 3% (Wilhelms et al, 1987)

Thus up until the end of the 1980's, all research on the auto-venting technology involved alterations to existing full-scale turbine runners. Using such installations to perform research is relatively expensive, and only minor variations

could be tested. Limited research in water tunnels was combined with what had been

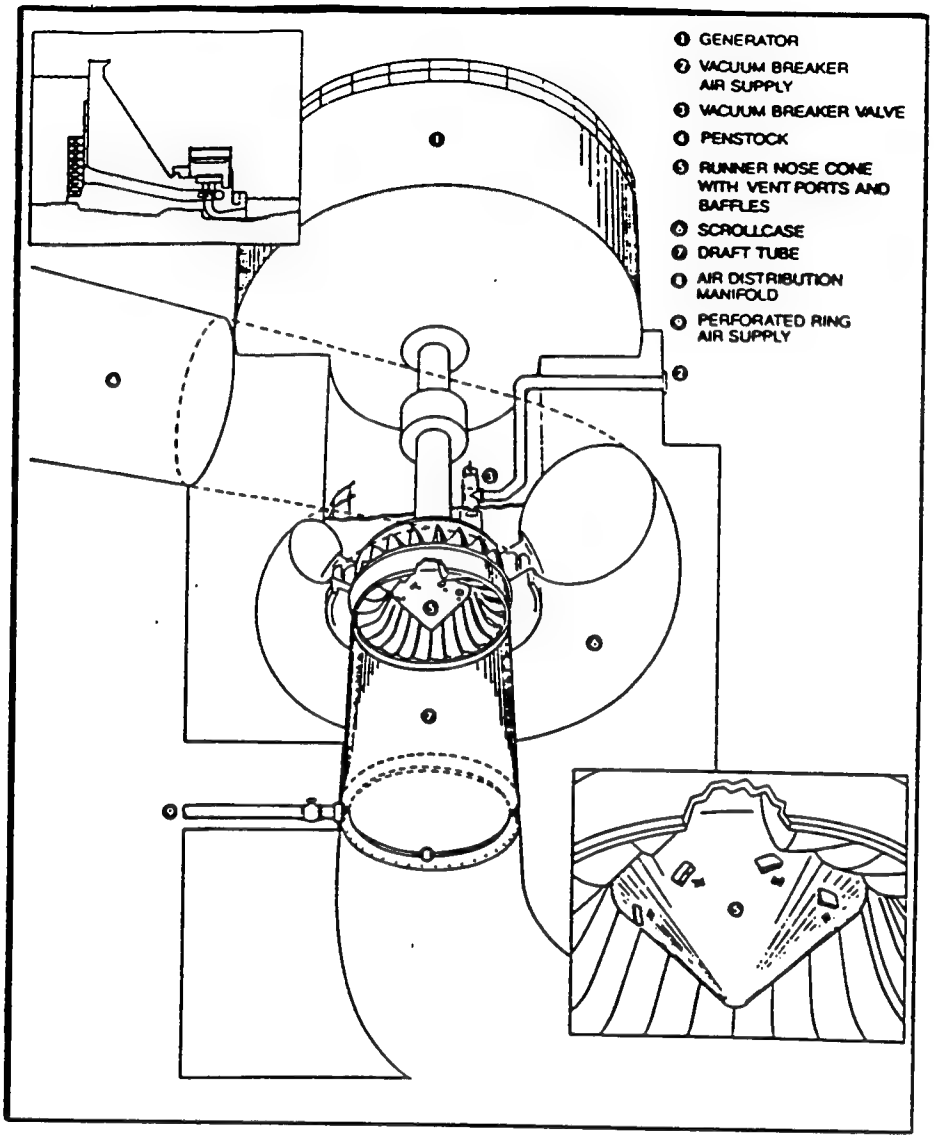

Figure 2.1 A view of a Francis turbine showing various locations baffles can be placed in an aeration system. The insert shows baffle placement on the runner nose cone.
(Bohac and Ruane, 1990)

successful previously to design the required auto-venting alterations to an existing hydro turbine. The testing of major variations to previous designs required that a hydroturbine model be utilized, where access to the rotating machine could be accomplished easily and a number of alternatives could be tested at a lower expense than on a full-scale installation. Unfortunately, the research funds for such an undertaking were still significant, and were not available. With a large number of hydroturbine runners scheduled for replacement in the 1990's, the TVA saw an opportunity to perform the auto-venting tests simultaneously with the model tests required to estimate the efficiency of the new turbine runner.

TVA recently initiated a long term program to develop the auto-venting turbine and associated technologies. TVA will act as coordinator and liaison between several research oriented agencies including the U.S. Army Corps of Engineers, the U.S. Bureau of Reclamation, and Voith Hydro. TVA itself is acting to create a data base for reaeration and auto-vented turbine operational characteristics. Other responsibilities taken on by TVA include model and prototype performance evaluations, development of numerical formulations for two phase flows, and development of scaling techniques to predict prototype behavior from model results (Mobley and Brice, 1991). Through a contract to the University of Iowa, they are also adapting a numerical flow model developed for the U.S. Navy to provide coordinates for flows through various cross-sections and curvatures, and ultimately to compute the flow details through the turbine.

The U.S. Army corps of engineers, as a part of this project, will provide TVA with a model for correlating laboratory and field data on DO uptake, air concentrations, air/water contact time, and DO deficits. The research was contracted to the University of Minnesota, and will result in a model/full-scale similitude relationship for oxygen transfer. The research performed at the University of Minnesota is the subject of this thesis. Furthermore, the Waterways Experiment Station is investigating turbulence effects on bubble size distribution, gas transfer, and prototype scaling using a numerical model (March et al, 1991)

Replacement of the hydroturbine runners operated by the U.S. Army Corps of Engineers will begin 5 to 8 years after the replacement program of TVA. Because many of these sites could benefit from the use of AVT technology, the U.S. Army Corp of Engineers is an enthusiastic partner in the AVT research program.

The U.S. Bureau of Reclamation is supporting the effort through the use of the Grand Coulee model test stand at Colorado State University. This will provide another set of auto-venting test data which can be compared to the Norris tests. The Grand Coulee model tests, however, will not be useful for a similitude relationship unless similar tests are performed on the full-scale installation.

III. Data Analysis

A. Mass Conservation

The basis for this analysis of auto-venting turbine data, and eventual development of a scaling relation, is mass conservation. The mass conservation equation applied to bubbles in a liquid takes the following form in the Lagrangian reference frame:

$$\frac{dC}{dt} = K_L' \frac{A'}{V}(C_S - C) \tag{3.1}$$

where C = the mean concentration of dissolved oxygen in the water, measured in the control volume,
t = time,
K_L' = the liquid film coefficient for bubble-water oxygen transfer, which is a function of time,
A' = the surface area of bubbles, also a function of time,
V = control volume corresponding to A and C measurements, and
C_s = the saturation concentration at equilibrium between the bubble and water.

Assuming that C_s remains constant, equation 3.1 can be integrated to give

$$-\ln\left[\frac{C_S - C_U}{C_S - C_d}\right] = \int_{t_d}^{t_u} K_L' \frac{A'}{V} dt = K_L \frac{A}{V} t \tag{3.2}$$

where C_u and C_d are concentrations measured upstream of the point of ventilation, and downstream of the location where the bubbles leave the flow (tailwater) respectively, and t is the residence time of the bubbles in the flow, or the time of

contact. K_L and A are mean values of K_L' and A', weighted by their impact on bubble-water oxygen transfer.

If we define transfer efficiency as

$$E=\frac{C_d-C_U}{C_S-C_U} \tag{3.3}$$

and we define a specific surface area as

$$a=\frac{A}{V} \tag{3.4}$$

then equation 3.2 can be rewritten in the following form:

$$-\ln(1-E)=K_L a t \tag{3.5}$$

Thus a factorial increase in liquid film coefficient, interfacial surface area, or in residence time will cause the term -ln(1-E) to increase by the same factor. In addition, because equation 3.5 is developed from the mass conservation equation (eq. 3.1) it will perform properly at the two limits for oxygen transfer efficiency: as $E \rightarrow 0$, $-\ln(1-E) \rightarrow 0$, which corresponds to $K_L at \rightarrow 0$; as $E \rightarrow 1$ (100% transfer), $-\ln(1-E) \rightarrow \infty$, which corresponds to an infinite value of $K_L at$. The term -ln(1-E) will therefore be used in an analysis of the model and full-scale oxygen transfer data.

B. Model Studies

1. AVT Runner Model

TVA recently funded Voith Hydro and American Hydro to propose and evaluate alternative designs for turbine runners to increase aeration and to estimate the operating efficiencies of the replacement runners. The alternatives include a redesigned Francis turbine hub with baffles and injection ports behind the baffles as well as at the thrust relief valves and deflectors, turbine runner blade trailing edge air injection, a coaxial diffuser, discharge ring injection, a snorkel tube, and combinations of these alternatives, as illustrated in figure 3.1 (March et al. 1991). TVA and Voith Hydro are co-funding extensive model studies of these alternative runner designs. Effects being investigated are air flow, aeration performance, efficiency, cavitation, runaway speed, and pressures and pressure fluctuations. Dimensional analysis and prototype comparisons will be used for performance scaling criterion.

One of the two turbine test stands at Voith Hydro's S. Morgan Smith Memorial Hydraulic Laboratory in York, Pennsylvania, is being used for the current studies of these AVT designs (figure 3.2). The stands each have a head tank, penstock, test section, tail tank and dynamometer, and share a 120,000 gallon reservoir, two service pumps and a single control room.

Performance tests were conducted at the Voith Hydro test stand between

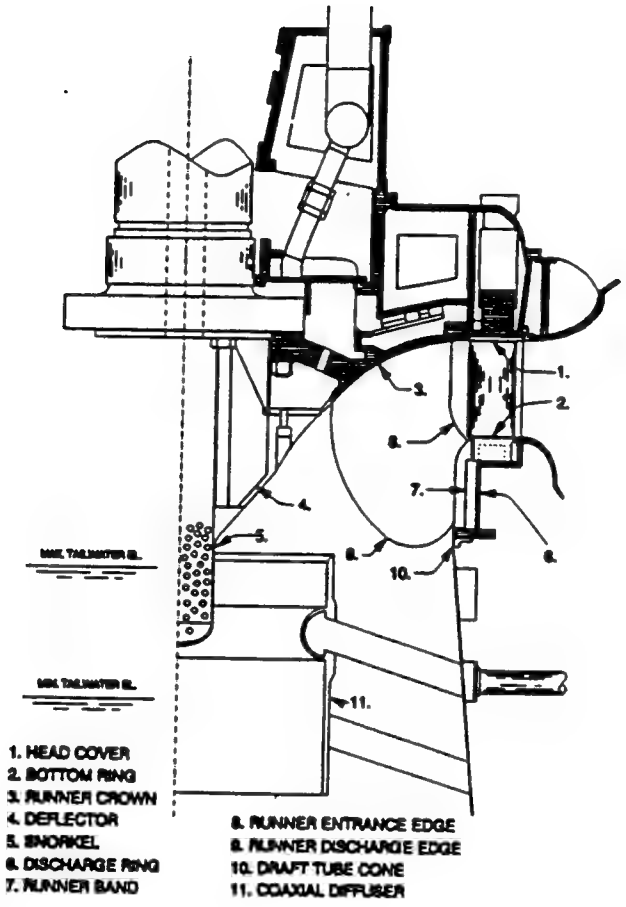

Figure 3.1 Several venting locations for turbine aeration (March et al, 1991)

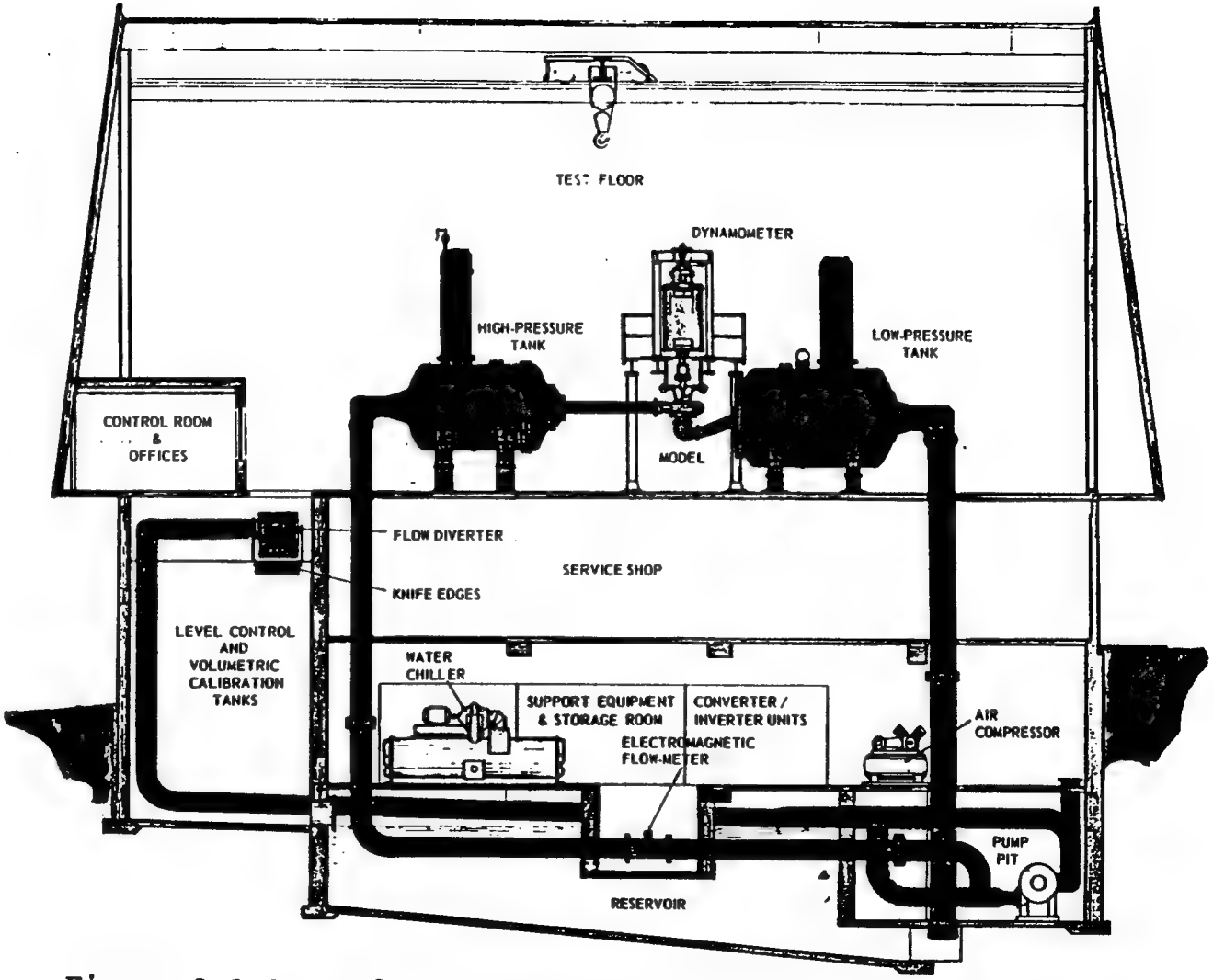

Figure 3.2 General arrangement of Voith's S. Morgan Smith Memorial Hydraulic Laboratory Turbine test stand (Mobley et al, 1990)

December of 1990 through July of 1991. The model tested was an 11.71 scale model of TVA's Norris dam hydroturbine. The turbine model was tested over the required full-scale operating head range of 130 to 190 feet for air admission and oxygen transfer at 20 combinations of gate settings between 12 and 24.675 mm (representing full gate) with rotational speeds ranging from 385 to 1300 rpm. The model runner was equipped with hub baffles to accurately represent the prototype runner installed at Norris Dam. Rotational speeds of 385, 900, 1028, 1100, 1133, 1148, 1170, and 1300 rpm were evaluated in terms of oxygen transfer efficiency with respect to increasing gas void ratio.

2. Difficulties Encountered in the Model Tests

Because the auto-venting turbine operates with two-phase flow, difficulties were encountered in attempting to measure predicted turbine performance and DO increase with the Voith turbine test stand which was designed to model only single-phase flows.

From the standpoint of mass transfer from bubbles, pressure is of significant importance. High pressures will increase the concentration of oxygen (in mg/l) in the bubble and will in part control the size of coalescing bubbles. This will have complex effects on the mass transfer as increased bubble size decreases the overall contact area for mass transfer, while an increased concentration in the air would increase the concentration gradient between the air and water phases and seek to increase the oxygen transfer. Since pressure in the draft tube of the full-scale facility is changing relatively rapidly, these processes have varying degrees of influence as the flows move downstream. Insufficient information was available to determine the proper oxygen saturation concentration to use in analyzing the full-scale and the model tests. This is a source of potential error in the resulting analysis, which assumed that the oxygen saturation concentration, C_s, was at local atmospheric pressure. Suggestions on further tests to determine a more appropriate value of C_s are made in the Conclusions and Recommendations sections.

3. Evaluation of AVT Model Test Results

The model test data was compiled by TVA and sent to the University of Minnesota for evaluation. The data was manipulated to show the effects of rotational speed, gas void ratio, and gate opening on gas transfer efficiency.

Gas transfer efficiency, as stated earlier is a function of the DO deficit between the upstream and downstream lengths of the control section as well as the saturation (equilibrium) concentration of oxygen in the water. Upstream and downstream DO concentrations corresponding to scroll case and tail tank locations respectively, were provided in the model test data. DO saturation concentrations were calculated using the following equation (Hua, 1990)

$$C_S = \frac{P}{P_0}[14.562 - 0.41022T + 0.007991T^2 - 0.000077774T^3] \qquad (3.6)$$

where C_s = saturation concentration of oxygen in mg/l
P = local absolute pressure,
P_0 = atmospheric pressure at sea level in the same units as P, and
T = water temperature in °C.

Temperature values for the water in the test stand were provided in the data compiled by TVA. Pressure values were taken from measurements taken in the model tail tank. The pressure values were assumed to be valid and without major variances between the turbine runner and the draft tube exit.

Gas void ratio was defined as the relative flow rate of air with respect to the total flow rate

$$\phi = \frac{Q_{air}}{Q_{air} + Q_{water}} \tag{3.7}$$

where ϕ = gas void ratio expressed as % by volume,
Q_{air} = volumetric flow rate of air under standard conditions,
Q_{water} = volumetric flow rate of water.

As will be discussed in section IV, the theory described here results in a linear dependence between specific surface area and gas void ratio (ϕ). There should therefore be a linear relation between -ln(1-E) and ϕ as described by equation 3.5. Figures 3.3a through 3.11a show the model test data for all the tested rotational speeds, given as -ln(1-E) vs ϕ. A linear regression of the form $-\ln(1-E) = a\phi$ was developed from the data with the limit that when $\phi=0$, E=0. As can be seen by observing the regression line (center line running through the data), there is some data scatter for each test. However, the 95% confidence interval represented by the upper and lower lines, evaluated from the uncertainties in the slope and intercept of the linear regression, show a good normal distribution.

Figures 3.3b through 3.11b, represent the data and regression analysis for measured oxygen transfer efficiency (Em) and gas void ratio. Included in the figures are a best fit line from the regression analysis and lines representing the upper and

lower limits of a 95% confidence interval. In these cases the regression line has a parabolic shape with an asymptote at E=1.0 (100% transfer). The regression lines are summarized in table 3.1. Figures 3.4a and 3.4b showing model data at 900 rpm are inconsistent with figures 3.5a and 3.5b, also at 900 rpm. It is suspected that there is an experimental bias in the data shown in figures 3.4a and 3.4b. Therefore, only the data represented in figures 3.5a and 3.5b will be used for evaluation of the similitude criterion.

Figure 3.12 shows the effect of rotational speed upon oxygen transfer efficiency. The curves shown represent oxygen transfer efficiency at constant gas void ratios calculated from the linear regressions expressed in figures 3.3 - 3.11. The similitude theory that will be developed herein predicts an increase in transfer efficiency with rotational speed. It can be seen that there is also a distinct loss in efficiency above a critical rotational speed near 1100 rpm. It is hypothesized that this efficiency loss is due to the increasing axial flow velocity, resulting in residence times insufficient to allow bubbles to shear down to their minimum size. The result is that quantities of air pass through the turbulent vertical section of the draft tube without attaining the maximum specific surface area, therefore limiting oxygen transfer in the draft tube. Table 3.2 shows the decrease in draft tube residence time with increasing rotational speed.

The effect of wicket gate opening upon transfer efficiency was determined by

examining data for model operation at peak power production efficiency, corresponding to little or no swirl in the draft tube, and operation at gate settings above and below peak setting, corresponding to positive and negative draft tube swirl. As shown in figures 3.13 - 3.15, and summarized in table 3.3, relatively little change in transfer efficiency at the different gate settings are evident in the data. It was therefore surmised that swirl had little or no effect upon oxygen transfer efficiency.

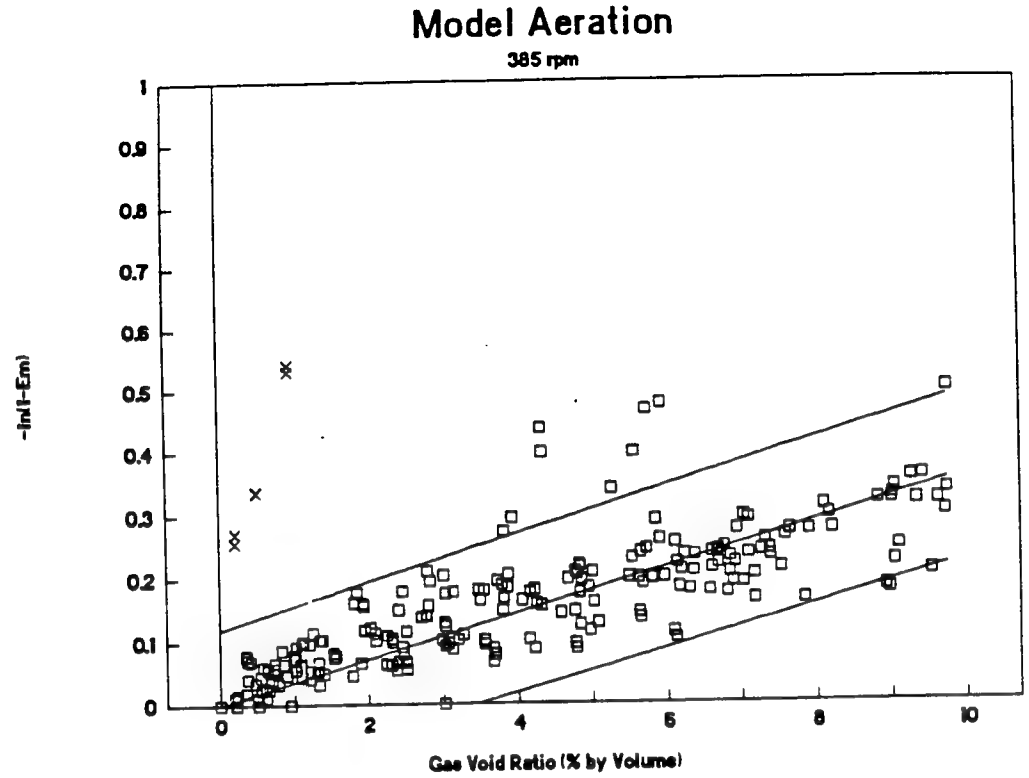

Figure 3.3a Model Aeration at 385 rpm. The data noted by an 'x' was excluded from the regression. The middle line represents the best fit regression. The outer lines correspond to the 95% confidence interval of the regression.

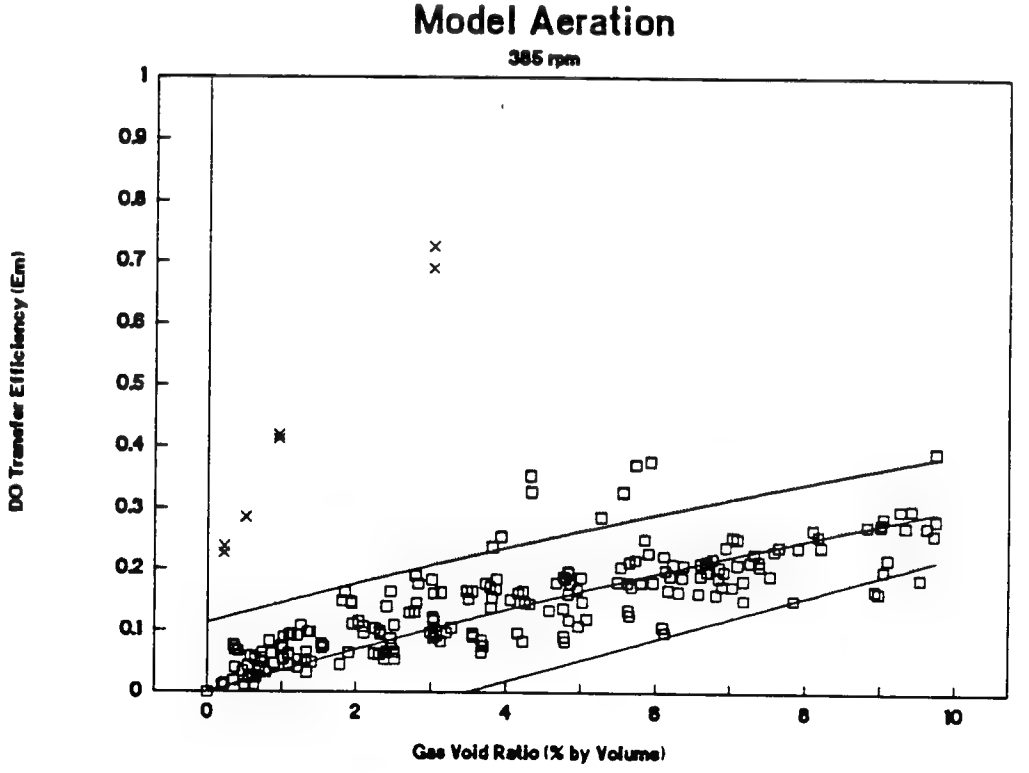

Figure 3.3b

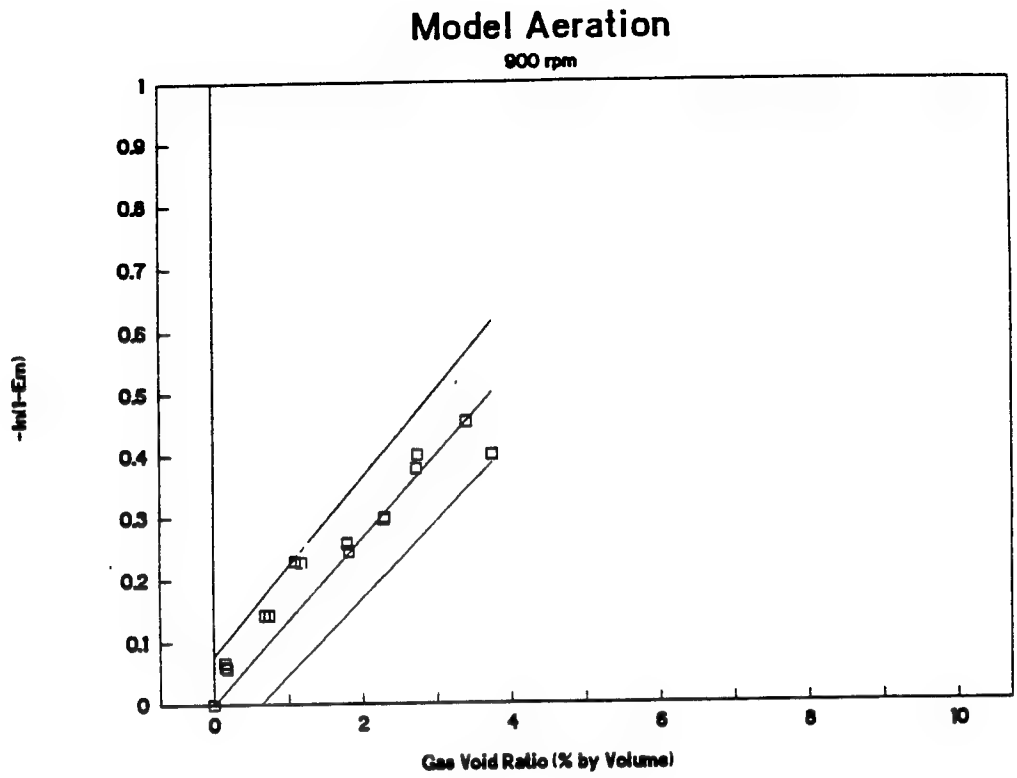

Figure 3.4a

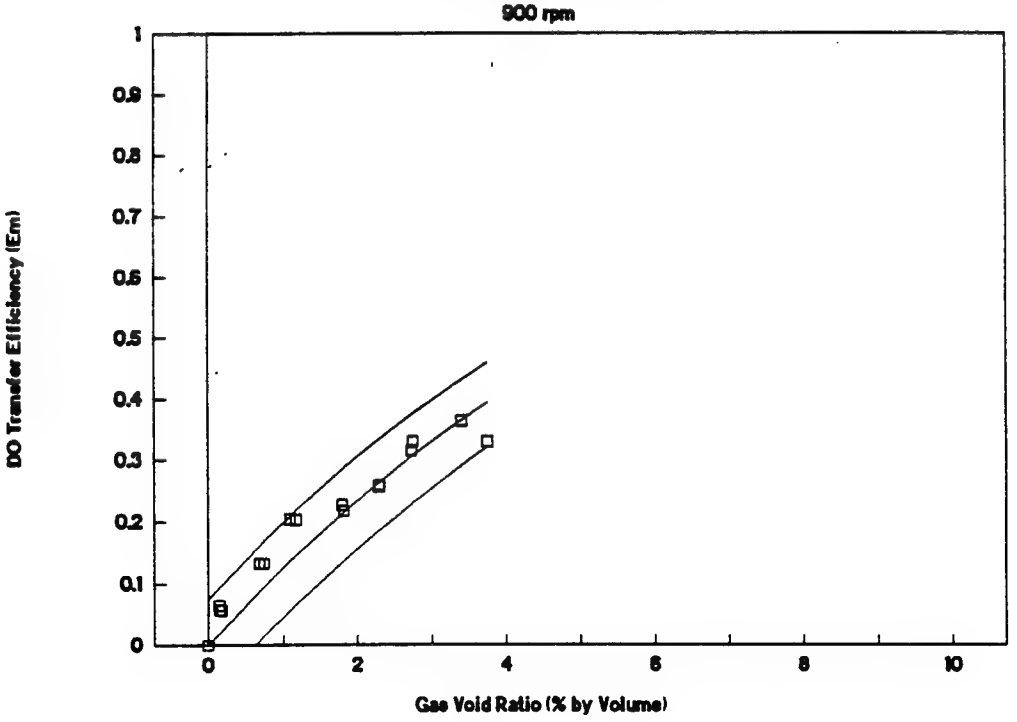

Figure 3.4b

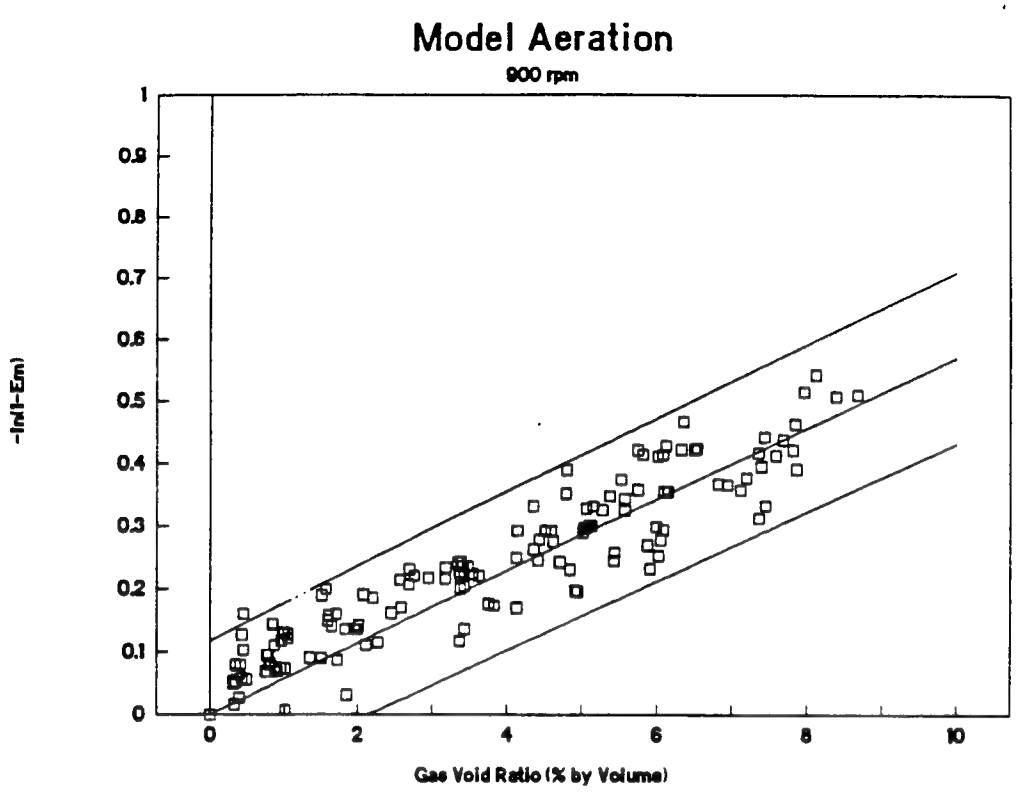

Figure 3.5a

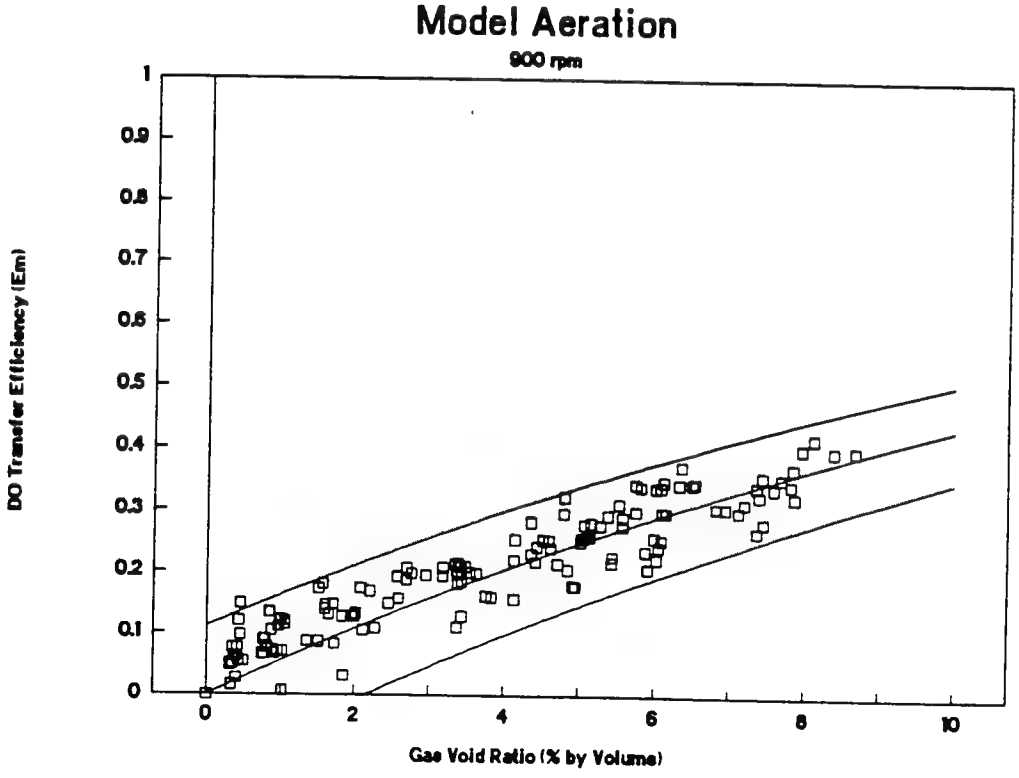

Figure 3.5b

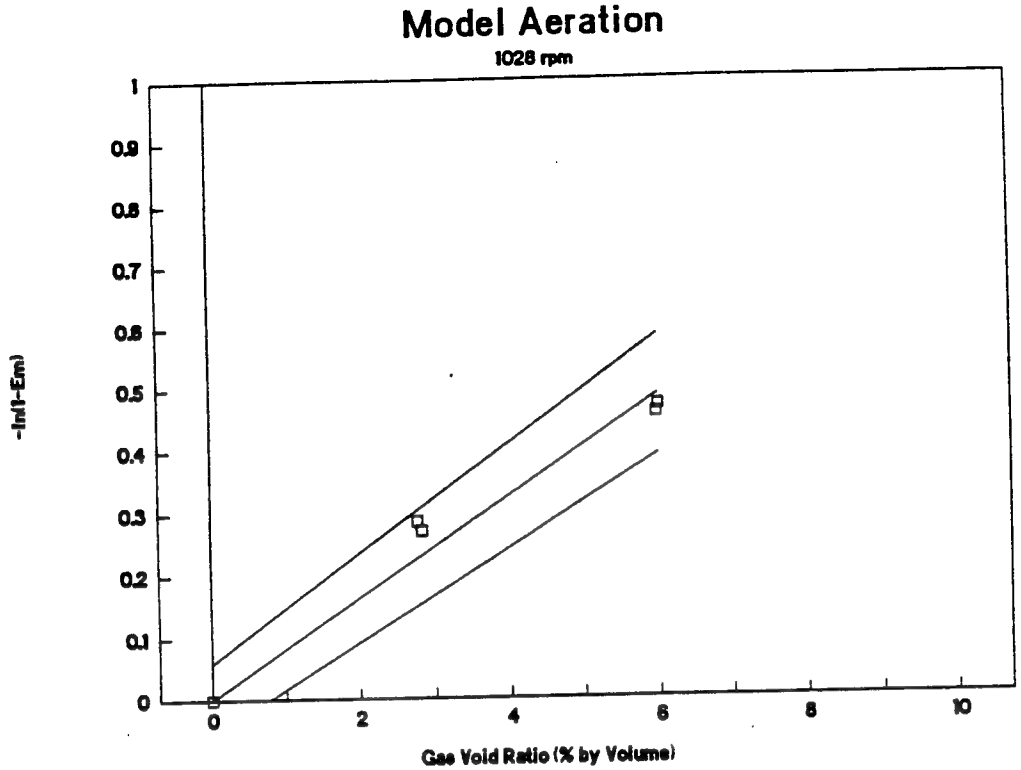

Figure 3.6a

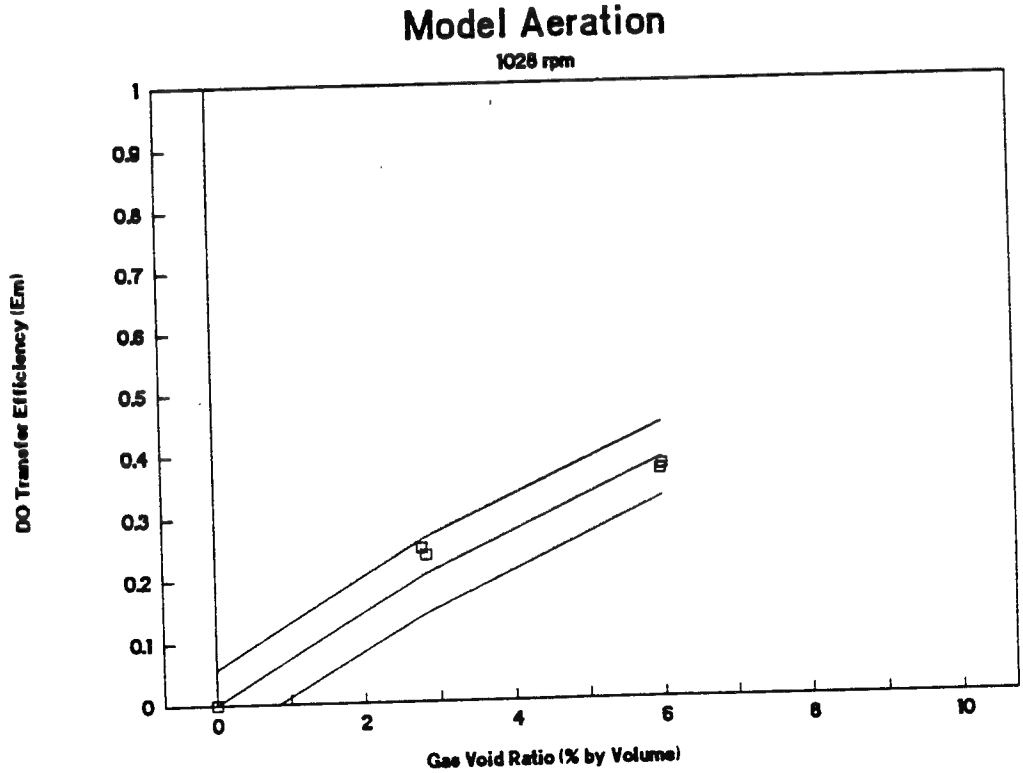

Figure 3.6b

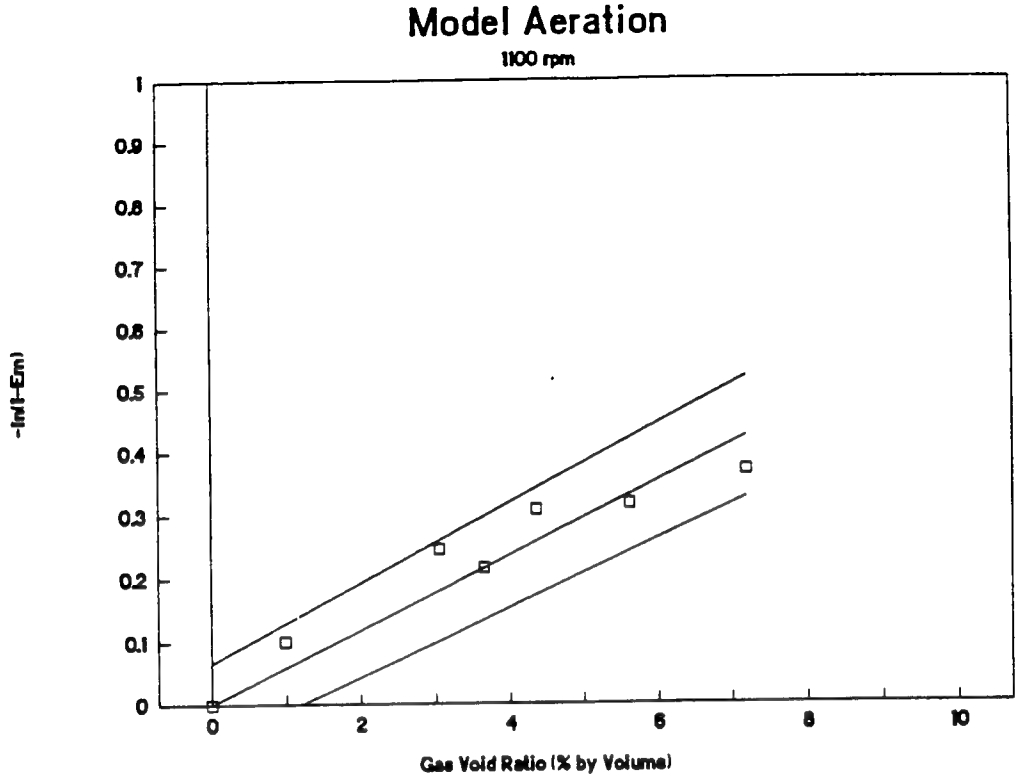

Figure 3.7a

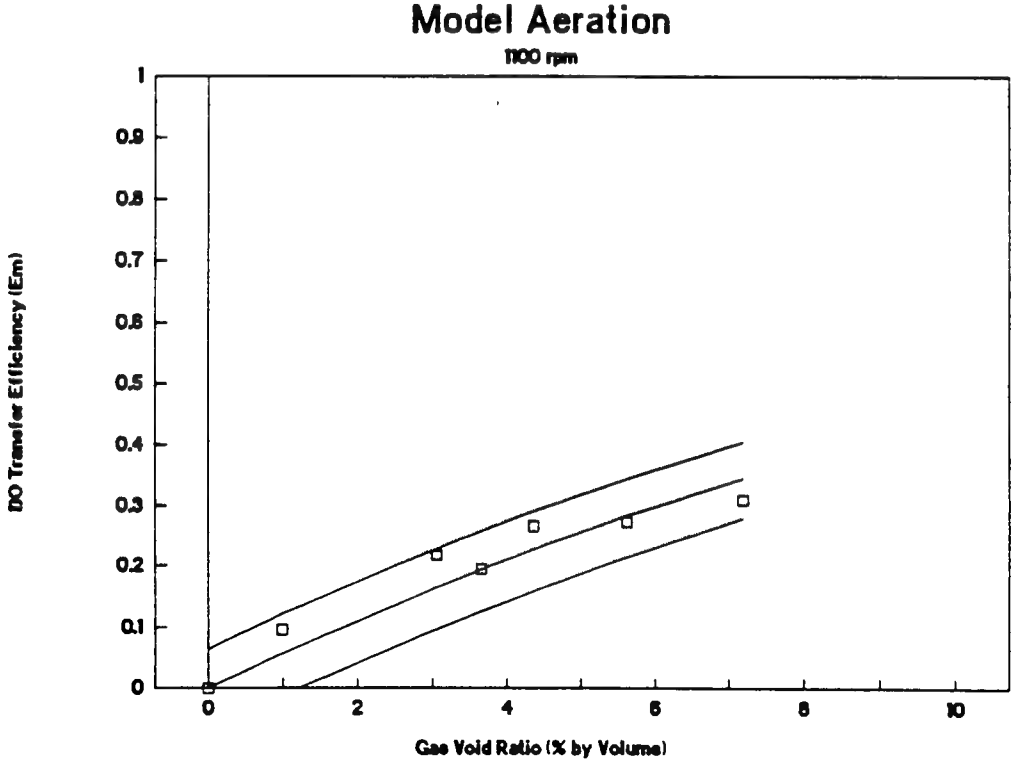

Figure 3.7b

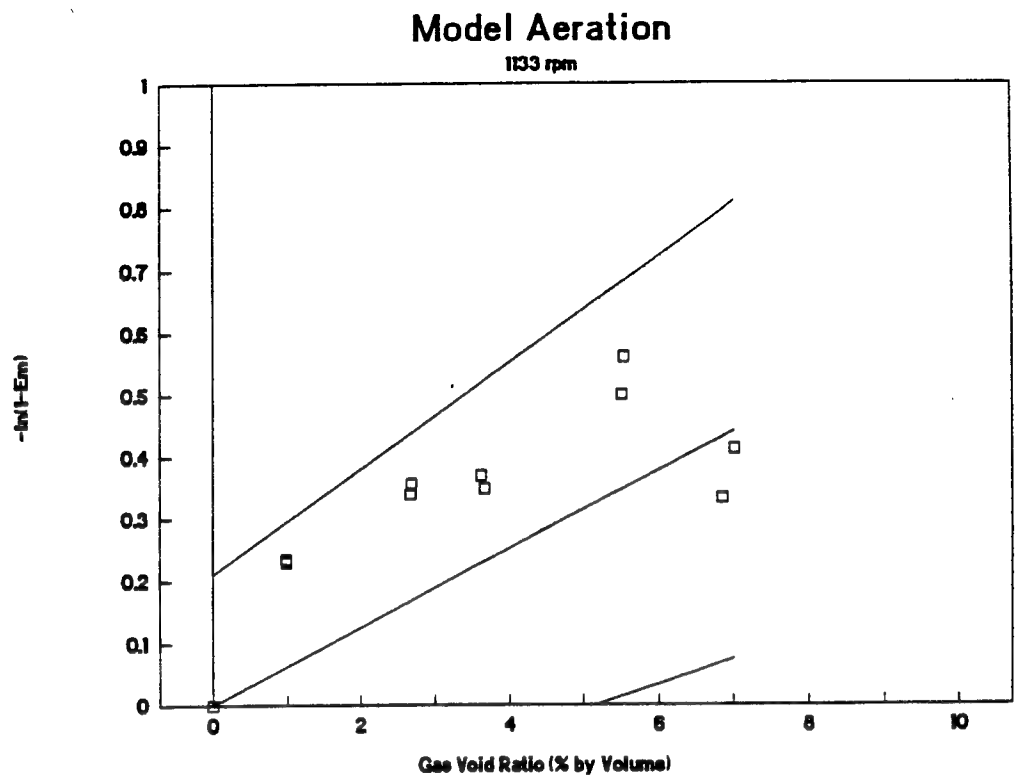

Figure 3.8a

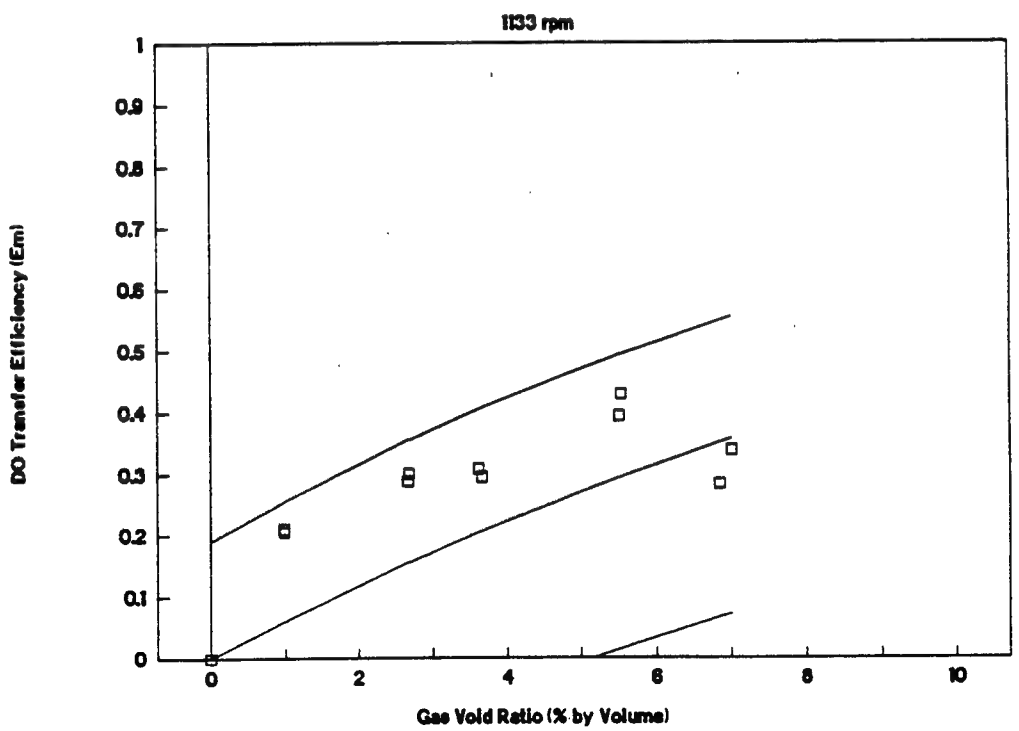

Figure 3.8b

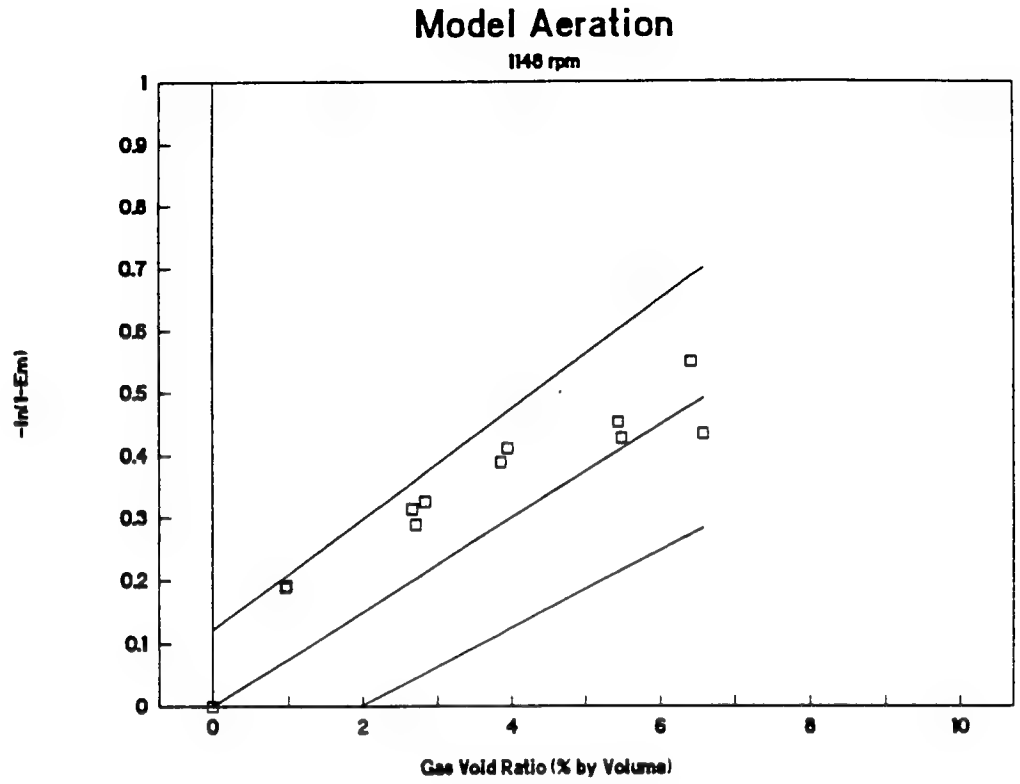

Figure 3.9a

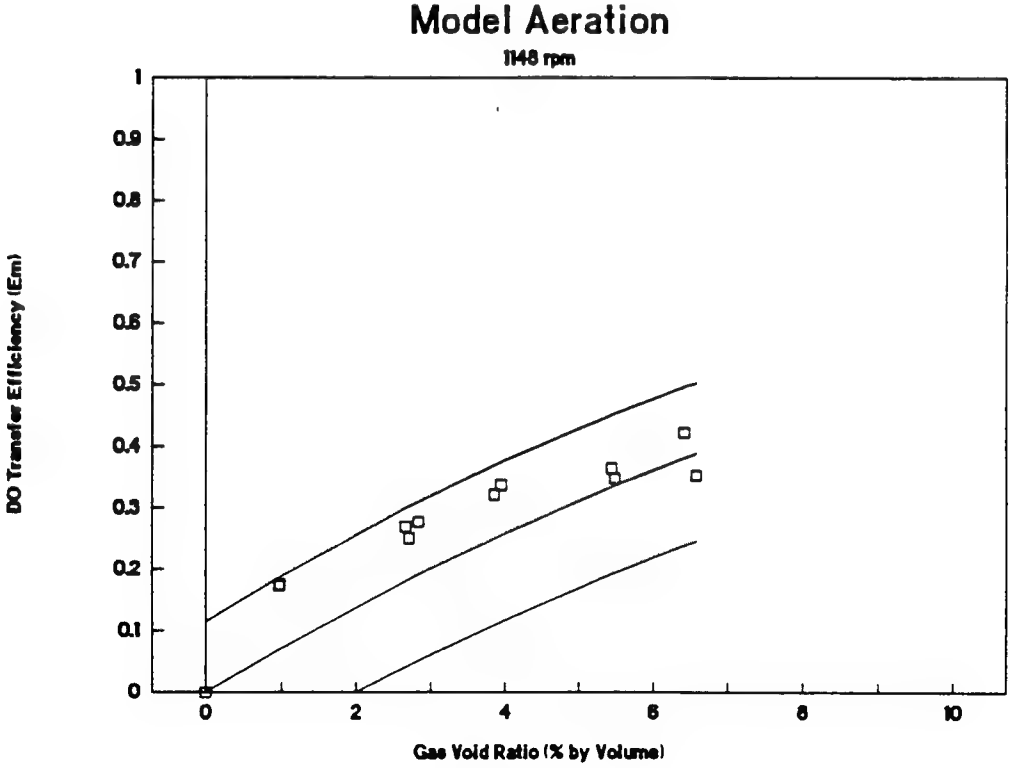

Figure 3.9b

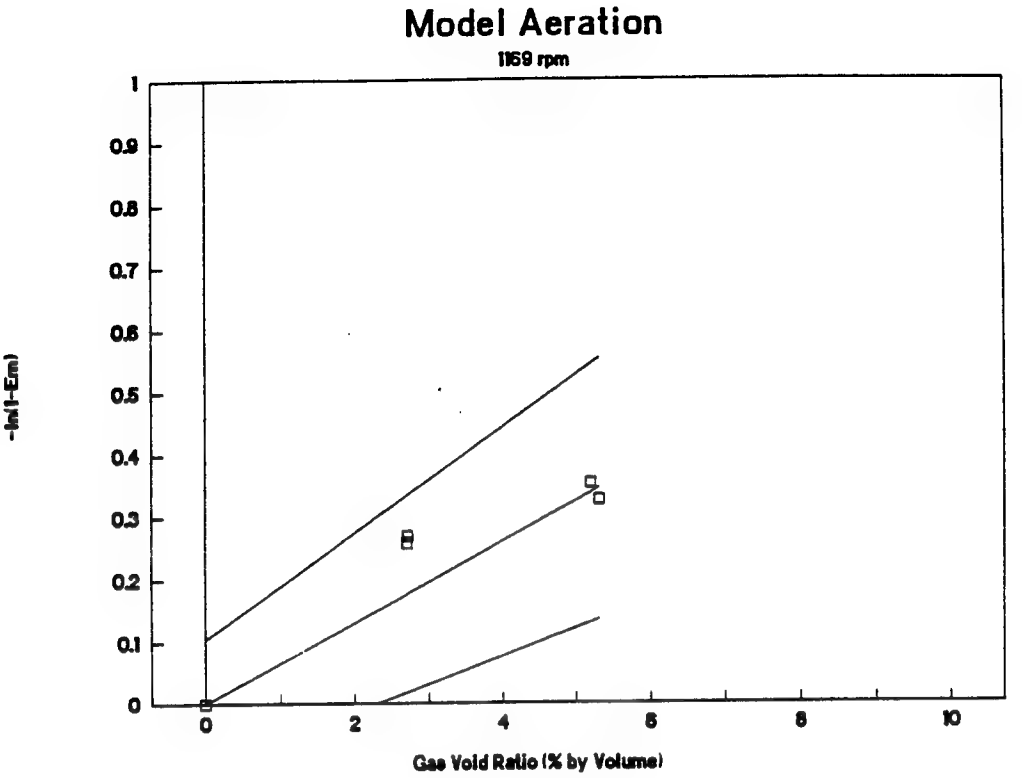

Figure 3.10a

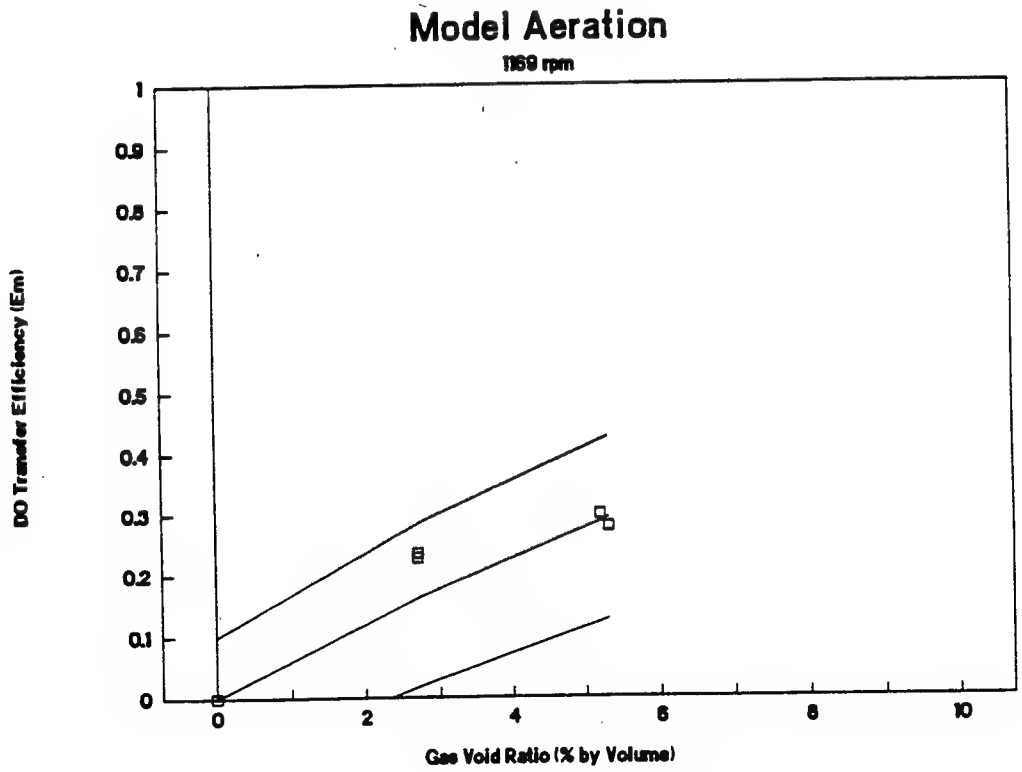

Figure 3.10b

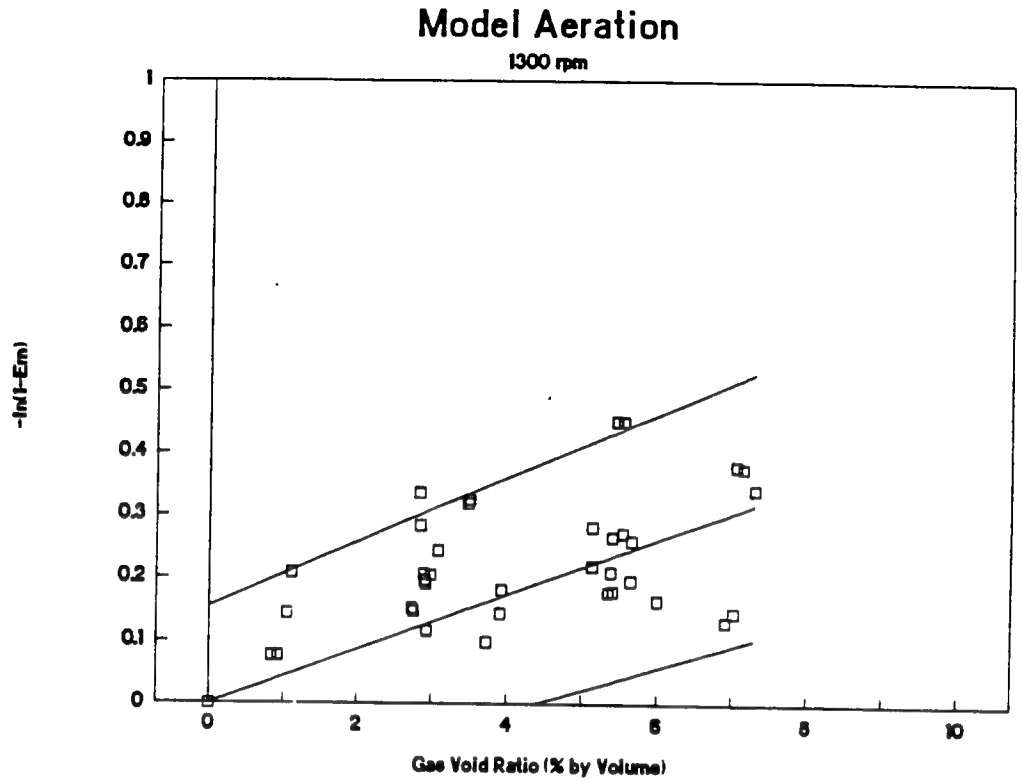

Figure 3.11a

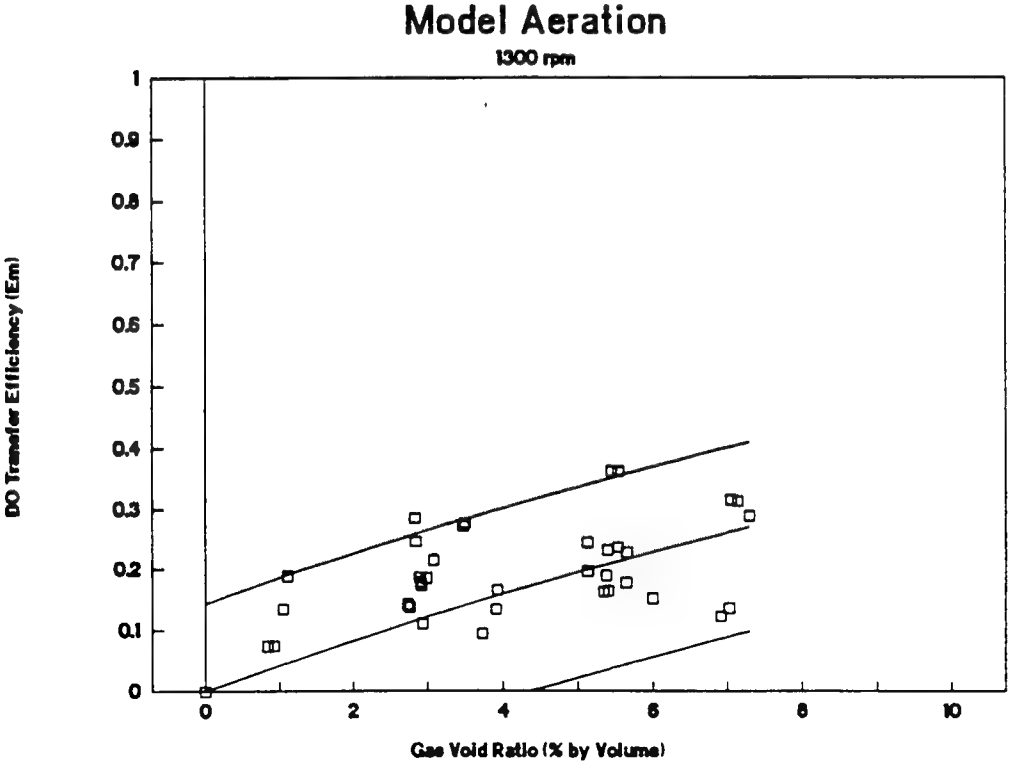

Figure 3.11b

Table 3.1

Slopes and uncertainties for model data fit to the equation $-\ln(1-Em) = a\phi$ as represented in figures 3.3a - 3.11a.

Rotational Speed	Transfer Slope	Slope Uncertainty	Intercept Uncertainty
385	0.03576	± 0.00079	± 0.05930
900	0.05706	± 0.00104	± 0.05896
1028	0.08132	± 0.00315	± 0.02950
1100	0.05896	± 0.00209	± 0.03325
1133	0.06300	± 0.01118	± 0.10509
1148	0.07475	± 0.00669	± 0.06057
1169	0.06494	± 0.00992	± 0.05219
1300	0.04320	± 0.00398	± 0.08244

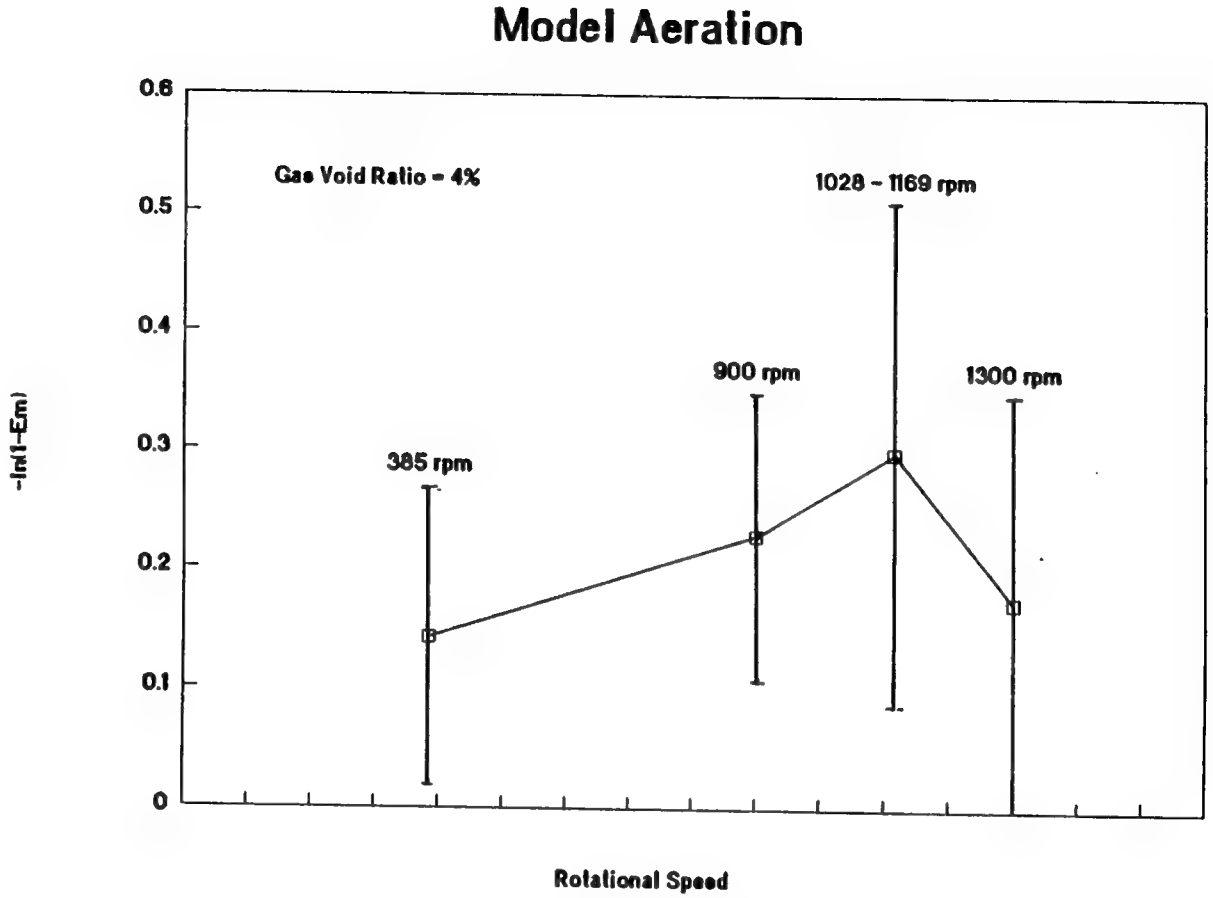

Figure 3.12 The effect of Rotational Speed on Oxygen Transfer Efficiency

Table 3.2

Model Turbine Draft Tube Residence Times for Vertical Discharge Section

Rotational Speed (rpm)	Axial Velocity (m/s)	Residence Time (sec)
385	0.472	0.474
900	1.077	0.222
1028	1.246	0.180
1100 - 1169	1.373	0.163
1300	1.581	0.151

Additional test descriptions referring to hydroturbine operational characteristics can be found in the Model Test Report for Norris Dam Aeration compiled by Voith Hydro and the Tennessee Valley Authority (Cybarluz et al, 1991).

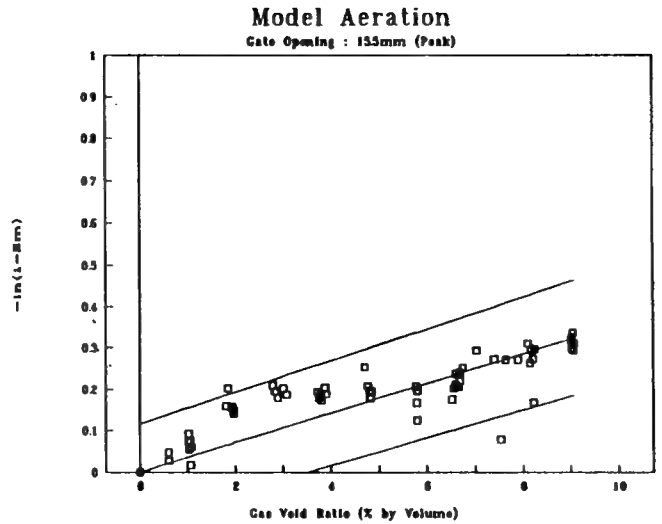

Figure 3.13

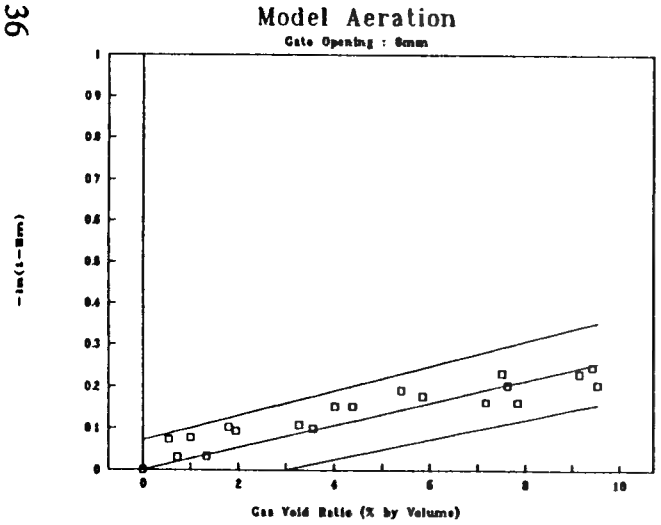

Figure 3.14

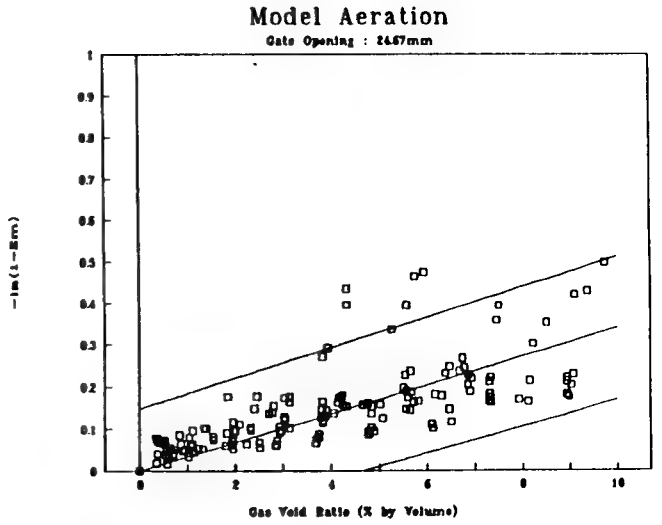

Figure 3.15

The effect of Gate Opening on Oxygen Transfer Efficiency

Table 3.3

Slopes and uncertainties for model data at 385 rpm fit to the equation $-\ln(1-Em) = a\phi$ as represented in figures 3.13 - 3.15.

Gate Opening	Transfer Slope	Slope Uncertainty	Intercept Uncertainty
8.0 mm	0.02690	± 0.00142	± 0.03554
15.5 mm	0.03569	± 0.00128	± 0.05803
24.67 mm	0.03404	± 0.00117	± 0.07395

C. Full-Scale Studies at Norris Hydroplant

1. Test Conditions

Aeration tests were performed at TVA's Norris Dam for purposes of testing operational performance as well as for verifying scaling and similitude relations developed from the model data. The Norris turbines operate at a rotational speed of 112.5 rpm, with an N11 speed (unit speed under 1 meter of head and 1 meter diameter) of 66, and a design head of 190 ft. The Norris turbine runner is an existing runner retrofit with vents and hub baffles. Figure 3.16 shows a schematic representation of the hub baffle aeration system. While the vacuum-breaker system in this installation was left intact, a bell-mouthed standpipe was installed as described by Wilhelms et al (1987), illustrated in figure 3.17, for increased air supply.

Preliminary tests of bolt-on streamlined baffles indicated significant aeration increases with a minor loss in operational efficiency. At the most efficient wicket gate opening, air-flow/water-flow volume ratios were in the range of 3%, resulting in DO increases of up to 3.0 ppm. The baffles themselves, without auto-venting, resulted in unit generating efficiency losses of less than 0.5% which translated into a power loss of less than 1 MW (Harshbarger, 1984).

Oxygen sampling was performed by TVA engineers and technicians in the

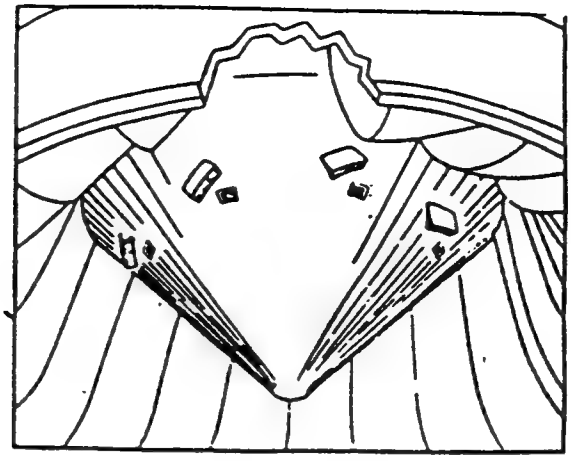

Figure 3.16 Distribution of baffles on the hub of Norris unit #2
(Wilhelms et al, 1987)

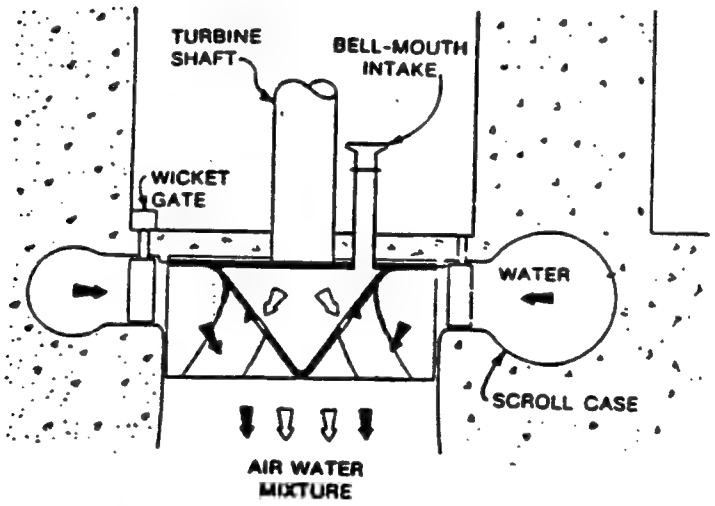

Figure 3.17 Large diameter bell-mouth air intake used at Norris dam
(Wilhelms et al, 1987)

penstock region as the upstream location and from a boat in the tailrace as the downstream location. As with most full-scale installations, there were difficulties associated with sampling oxygen concentrations, in addition to the expenses, effective access to the water conveyance facilities was limited.

A single tap in the penstock leading to an overflow chamber where a DO probe could be submerged was used as an upstream sampling location. Because hydroturbine intakes withdraw water from a large vertical cross-section of the reservoir the impacts of any existing stratification will be unknown to the upstream sampler. It is therefore quite likely that one tap along the penstock wall will not give a representative sample of the entire penstock cross-section, and the resulting concentration measurements will contain some unknown bias.

In the tailwater a DO probe was suspended on a weighted line from a boat piloted just below the turbine tail race bubble plume. Since the boat was constantly drifting about, it is possible that downstream sampling location with respect to the bubble plume was inconsistent, resulting in apparent changes in aeration performance as the probe measured different DO concentrations under the same circumstances. Additionally, when other turbines were in operation, typically not venting air, substantial cross mixing between discharge plumes could result in sampling error. The downstream measurement uncertainty would therefore be random in nature. The resulting precision uncertainty could be reduced by increasing the number of

measurement locations in the tailwater at each turbine setting.

In most cases, adjustments to the data can be made to account for the routine deviations in data taken at the full-scale installation if these measurement challenges are taken into account.

2. Full-Scale Test Results

The Tennessee Valley Authority ran tests on its Norris Dam Turbine unit #2 on three separate occasions. Figure 3.18 shows the raw oxygen transfer data received, using local atmospheric pressure in the computation of C_s. The data are tabulated in appendix A.

The oxygen transfer efficiencies for the data taken on 6–9–92 seem to be higher than those taken on either 10–10–82 or 6–29–83. It is believed that downstream sampling difficulties could explain the scatter in any individual test date, but not the consistent difference between two sampling dates. The use of atmospheric pressure to compute C_s also could not account for this difference because the same procedure was used for all test dates. The consistent differences in transfer efficiency could be explained, however, by a density stratification in the withdrawal zone of the reservoir that carried through into the penstock on 6–9–92. This would make the upstream sampling point unrepresentative of cross-sectional mean DO in the penstock, and result in a y-intercept in the $-\ln(1-E)$ vs ϕ plot that is significantly different from zero, as observed in figure 3.18 for the 6-9-92 data.

To determine the magnitude of oxygen transfer which occurred in the turbine draft tube, an examination of the data for tests where there was no air vented through the turbine was performed. In such circumstances, no oxygen transfer should occur within the draft tube. The upstream DO concentrations were therefore

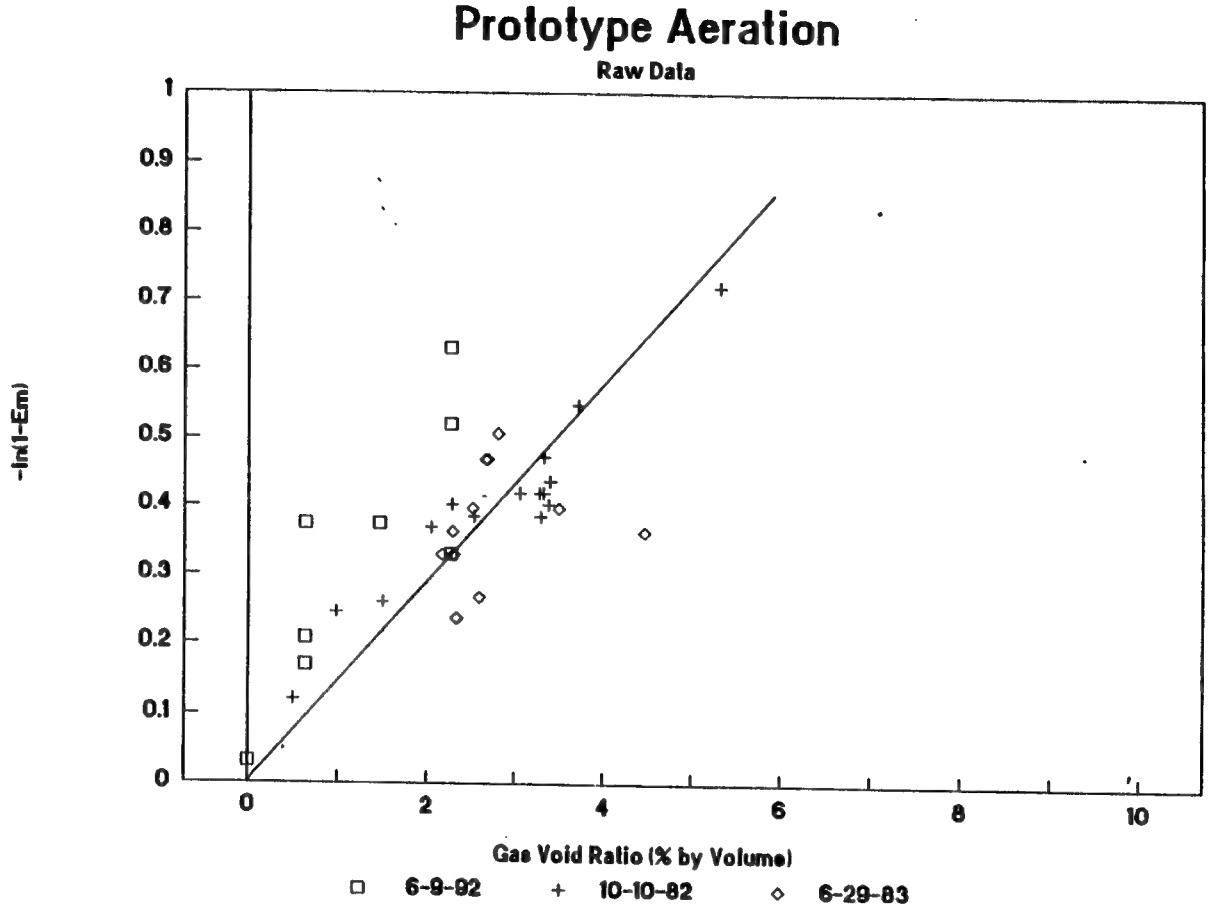

Figure 3.18 Aeration performance for Norris Unit #2

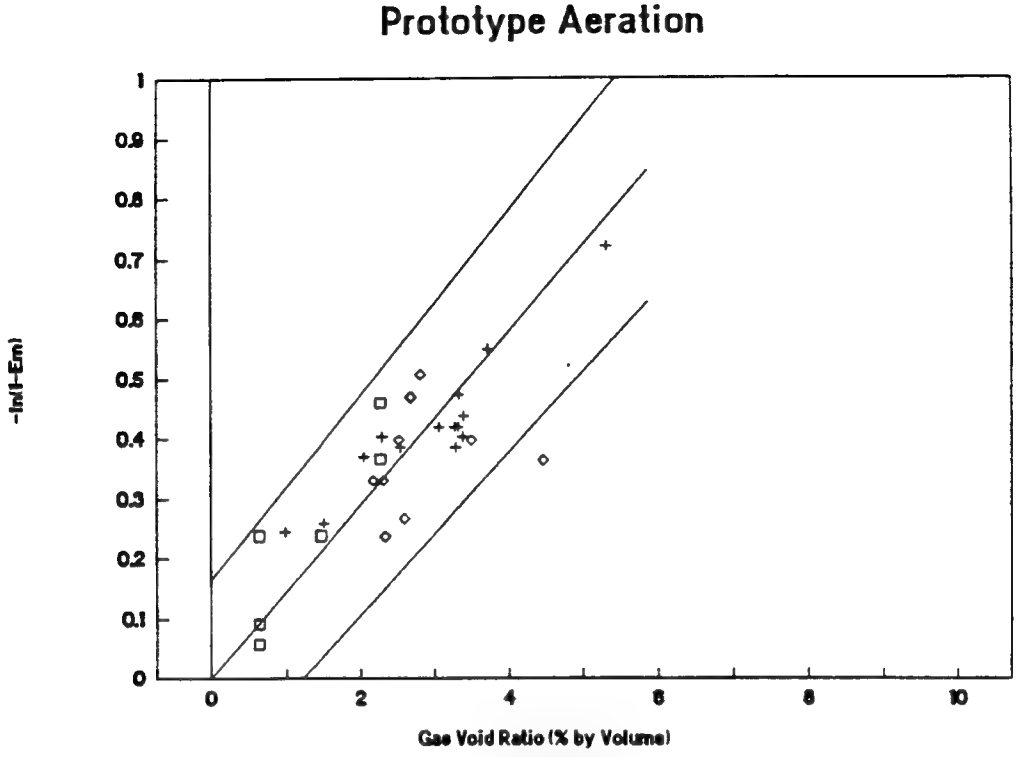

Figure 3.19 Measured prototype aeration performance. The slope of the curve fit is 0.1444 ± 0.0047 with an intercept uncertainty of ± 0.0824.

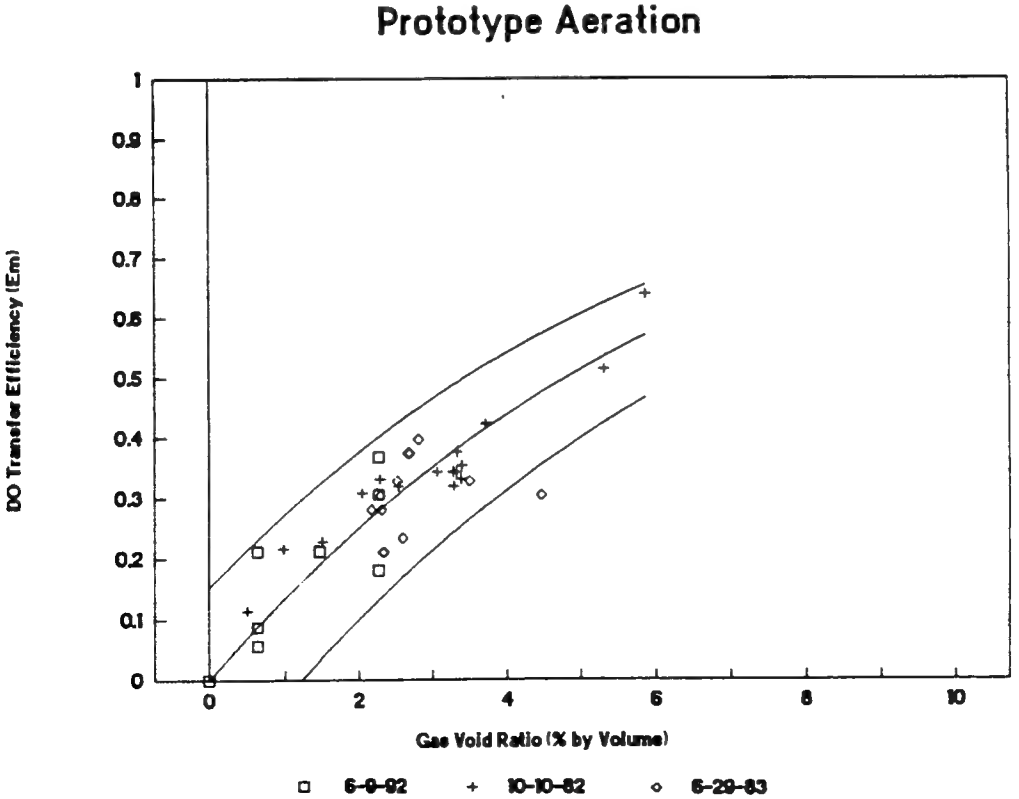

Figure 3.20 The curve-fit of Figure 3.19 plotted as measured Transfer Efficiency (Em) vs. Void Ratio.

assigned values equal to the downstream values. This adjustment ignores the possibility that the DO uptake in the tailrace boil can result in a 'no air' transfer efficiency of between 4 and 8 percent (Wilhelms et al, 1987). Adjustment of the data for 6–9–92 resulted in collapse of the data for all three tests, as shown in figure 3.19. Within the random scatter of the data, the three sets now show a single behavior pattern for the Norris installation.

As in the model data, there is a linear proportionality between ln(1-E) and the gas void ratio (ϕ). A linear regression of this logarithmic relation for the oxygen transfer efficiency data from the three full-scale tests vs void ratio is shown in figure 3.19 with the 95% confidence interval for the regression. Figure 3.20 shows the behavior of the oxygen transfer efficiency vs. gas void ratio, illustrating the exponential behavior of the data as predicted by the similitude relation. Note that there is a horizontal asymptote at E = 1.0 (100% transfer efficiency) denoting a maximum transfer efficiency. A slope of 0.1444 is shown in figure 3.19. This is significantly different from the slopes ranging from 0.035 to 0.081 for the turbine model.

IV. Similitude Theory

For similarity between a turbine model (subscript 1) and the full-scale turbine (subscript 2) equation 3.5 may be written for both model and full-scale as:

$$\frac{\ln(1-E_1)}{\ln(1-E_2)} = \frac{(K_L at)_1}{(K_L at)_2} \qquad (4.1)$$

To develop equation 4.1 into a more useful form, the liquid film coefficient, the specific surface area, and the time of contact will be investigated in detail separately.

A. Determination of a K_L Scaling Relationship

The standard surface renewal relation for the liquid film coefficient takes the form

$$K_L \propto \sqrt{Dr} \tag{4.2}$$

where D = the molecular diffusivity of the compound in water and
r = a renewal rate dependent upon system characteristics.

For the auto-venting turbine, r is a function of the shear velocity, which is approximately proportional to the axial flow velocity, and the kinematic viscosity of water

$$r \propto \frac{u^{*2}}{\nu} \propto \frac{U^2}{\nu} \tag{4.3}$$

where u* = the shear velocity of the flow,
U = the cross-sectional mean flow velocity in the axial direction, and
ν = the kinematic viscosity of water.

Substitution of equation 4.3 into equation 4.2 yields Levich's relation for K_L from bubbles rising in a quiescent fluid

$$K_L \propto \frac{D^{1/2} U}{\nu^{1/2}} \tag{4.4}$$

This equation is similar in form to one developed by Azbel (1981) which

applies to bubbles in a bubble swarm. He began with Levich's (1962) theoretical expression for the air-water mass flux from a spherical bubble

$$\frac{dm}{dt}=2\left[\frac{\pi D V_r}{d_b}\right]^{1/2} d_b^2(C-C_s) \tag{4.5}$$

where m = the mass of oxygen in the bubble,
D = the molecular diffusivity of oxygen in water,
v_r = the velocity of the bubble relative to the liquid phase,
d_b = bubble diameter,
C = concentration of oxygen in the bubble, and
C_s = the saturation concentration in the water.

Azbel then developed an expression for v_r in a turbulent flow field by assuming that the flow is composed of equal sized bubbles that are uniformly spaced. The relationship has a characteristic velocity and a characteristic length that are properties of the turbulent flow field (Azbel, 1981).

$$v_r=\frac{U^{3/2} d_b}{2(\nu L)^{1/2}}\frac{1-\phi}{(1-\phi^{5/3})^{1/2}} \tag{4.6}$$

where U = a characteristic velocity of the large eddies,
ν = kinematic viscosity of water,
L = a characteristic length of the large eddies, and
ϕ = the gas void ratio (air flow percentage by volume)

Substituting Azbel's equation and Levich's equation into the basic mass conservation equation given in section 3 and substituting in basic turbine similitude parameters yields the following scaling relation for the liquid film coefficient

$$K_L \propto \frac{D^{1/2} U^{3/4}}{\nu^{1/4} L^{1/4}} \frac{[1-\phi]^{1/2}}{[1-\phi^{5/3}]^{1/4}} \tag{4.7}$$

The important differences between equations 4.4 and 4.7 are the $U^{3/4}$ relationship developed in equation 4.7 opposed to the linear relation expressed in equation 4.4 and the fact that equation 4.7 contains a turbulent length scale. AVT gas void ratios are typically much less than 1, thus the importance of the ϕ terms in equation 4.7 would be very small and will hereafter be neglected.

Oxygen transfer in the auto-venting turbine cannot truly be described as having turbulence created only by rising bubbles, and certainly does not behave as a quiescent fluid. The turbulence is primarily from the high Reynold's number flow through the rotating machine. For that reason, it is possible that neither equation 4.4 or the bubble swarm theory proposed by Azbel and expressed in equation 4.7 properly parameterizes the liquid film coefficient for an AVT. A literature search provided no information that would be helpful to parameterize K_L in a highly turbulent bubble flow field. Therefore, equations 4.4 and 4.7 were empirically transformed, with attention given to units, into the following form (dropping the ϕ terms of equation 4.7)

$$K_L \propto \left(\frac{D U^{\beta}}{L^{2-\beta} \nu^{\beta-1}} \right)^{1/2} \tag{4.8}$$

where L = a characteristic length dimension of the large eddies, and
β = and empirical coefficient accounting for bubble swarm behavior in a turbulent flow field.

where equation 4.4 has $\beta = 2$ and equation 4.7 has $\beta = 3/2$.

For the auto-venting turbine, the characteristic velocity can be represented by the relations

$$U \propto \frac{Q}{A_{cs}} \propto \frac{n d_t^3}{d_t^2} = n d_t \tag{4.9}$$

where Q = the volumetric discharge of water,
A_{cs} = the cross-sectional area of the turbine runner, and
d_t = the diameter of the turbine runner.

Additionally, since the largest eddies are on the order of the runner diameter, the length scale in equations 4.6 and 4.8 can be represented by

$$L \propto d_t \tag{4.10}$$

Therefore, the scaling relationship between two homologous turbines for liquid film coefficients can be derived from equations 4.8, 4.9, and 4.10 as

$$\frac{K_{L1}}{K_{L2}} = \left[\frac{D_1}{D_2}\right]^{1/2} \left[\frac{n_1}{n_2}\right]^{\beta/2} \left[\frac{d_{t1}}{d_{t2}}\right]^{(\beta-1)} \left[\frac{\nu_2}{\nu_1}\right]^{(\beta-1)/2} \tag{4.11}$$

B. Development of a Scaling Criterion for Specific Surface Area

Since the specific surface area, a, is dependent upon the size of bubbles in the control volume it will be necessary to first determine the size of bubbles which occur in the turbine. The mean bubble diameter, d_b, for a shear flow in an auto venting turbine draft tube is a function of the maximum bubble size the shear forces will allow. Large bubbles, when introduced into the draft tube, are rapidly broken down by the shear forces in the flow, until the bubble size is sufficiently small that the surface tension forces are significant enough to restrict any further breakdown in bubble size.

Hinze (1955) experimentally studied the larger bubble sizes in rotating concentric cylinders and proposed that this bubble size is

$$d_m = k \left[\frac{\sigma}{\rho}\right]^{3/5} \epsilon^{-2/5} \qquad (4.12)$$

where d_m = the bubble diameter that encompasses 95 percent of the air by volume,
k = a constant of proportionality,
σ = surface tension,
ρ = density of water, and
ϵ = rate of turbulent kinetic energy dissipation per unit mass.

More recent experiments have confirmed the relationship proposed by Hinze. Sevik and Park (1973) examined jets issuing into water,and Killen (1982) studied the maximum stable bubble diameter in a boundary layer. In all cases the form of the

relation was found to be the same with the only difference being the value of the constant k. The difference in magnitude of the constant is partially due to the differing techniques used to determine ϵ, and also the different experimental setup.

The dissipation of turbulent kinetic energy is approximated by

$$\epsilon \approx \frac{q^3}{L} \tag{4.13}$$

where

$$q^2 = \frac{(\overline{u'^2} + \overline{v'^2} + \overline{w'^2})}{2} \tag{4.14}$$

with u', v, w = unsteady portion of the three velocity components, and
L = an integral eddy length scale of the larger eddies, which should be proportional to d_t.

Assuming that q scales with the velocity, U, equation 4.13 becomes

$$\epsilon \propto \frac{U^3}{d_t} \propto \frac{Q^3/d_t^6}{d_t} = \frac{Q^3}{d_t^7} \tag{4.15}$$

Therefore, equation 4.12 may be written as

$$d_m \propto \left[\frac{\sigma}{\rho}\right]^{3/5} \frac{d_t^{14/5}}{Q^{6/5}} \tag{4.16}$$

Because of the breakdown of larger bubbles created by the relatively high shear in a turbine draft tube, the distribution of bubble sizes versus bubble diameter will be relatively narrow. Gulliver et al (1990) used a photographic analysis of entrained

bubbles in a high shear flow to find that the volumetric mean bubble diameter was

$$d_b = 0.63 d_m \tag{4.17}$$

and the specific surface area was determined to be

$$a = 6.49 \frac{\phi}{d_m} \propto \frac{\phi}{d_b} \tag{4.18}$$

where ϕ = the gas void ratio, defined as

$$\phi = \frac{Q_{air}}{Q_{water} + Q_{air}} \tag{4.19}$$

where Q represents the respective flow rates of air or water.

Equation 4.18 is valid at the small gas void ratios normally found in an AVT. At higher gas void ratios, more complex relations are required to describe specific surface area (Azbel, 1981).

A scaling relation in the form of equation 4.11 can be developed from the insertion of equation 4.16 into equation 4.18

$$\frac{a_1}{a_2} = \left[\frac{\phi_1}{\phi_2}\right]\left[\frac{\rho_1}{\rho_2}\right]^{3/5}\left[\frac{\sigma_2}{\sigma_1}\right]^{3/5}\left[\frac{n_1}{n_2}\right]^{6/5}\left[\frac{d_{t1}}{d_{t2}}\right]^{4/5} \tag{4.20}$$

C. Contact Time

The contact time of the bubbles in the flow, t, is proportional to the length traveled between upstream and downstream measuring points divided by velocity. The length traveled should scale with runner diameter in homologous turbines. As mentioned previously, velocity scales as rotational speed times runner diameter.

$$t \propto \frac{d_t}{n d_t} \propto \frac{1}{n} \tag{4.21}$$

Or in similitude form,

$$\frac{t_1}{t_2} = \frac{n_2}{n_1} \tag{4.22}$$

D. Similitude Relation

Equations 4.1, 4.11, 4.20, and 4.22 can be combined and simplified into the following relation for gas transfer in homologous auto-venting turbines

$$\frac{\ln(1-E_1)}{\ln(1-E_2)}=\left[\frac{\phi_1}{\phi_2}\right]\left[\frac{D_1}{D_2}\right]^{1/2}\left[\frac{\nu_2}{\nu_1}\right]^{(\beta-1)/2}\left[\frac{\sigma_2}{\sigma_1}\right]^{3/5}\left[\frac{\rho_1}{\rho_2}\right]^{3/5}\left[\frac{n_1}{n_2}\right]^{(\beta/2+1/5)}\left[\frac{d_{t1}}{d_{t2}}\right]^{(\beta-1/5)} \qquad (4.23)$$

where β is an empirical coefficient to be determined in section V.

V. Empirical Fitting

Because of the loss in transfer efficiency at rotational speeds over 900 rpm it was concluded that there is some unknown bias within the data for the high rpm tests. As discussed in section III, this is conjectured to be due to insufficient residence time to allow sufficient bubble splitting in the high shear zones of the draft tube at high rotational speeds. As a result the similitude relation was only fit to the data for 385 rpm and 900 rpm. Fortunately, most of the oxygen transfer data on the Norris AVT model were taken at these speeds.

If the temperature dependent variables are removed from the similitude relation, the final result is a proportionality between transfer efficiency and gas void ratio, rotational speed, and runner diameter. Since scaling is performed at a given void ratio (ie. $\phi_1 = \phi_2$, in similitude format) the dependence drops to rotational speed and runner diameter. These two parameters in combination were used to determine the coefficient β.

The importance of rotational speed was found by scaling model data to other model operating conditions. As this removed the dependence upon runner diameter, the empirical fitting process was performed on a single variable, the exponent for rotational speed.

Having found the relative importance of rotational speed in the similitude

equation the model data for 385 rpm and 900 rpm was scaled to prototype operating conditions. As this involved a different runner diameter the exponent for d_t was found.

The final step, converting the known exponents to a single empirical coefficient was performed by referring to the individual components of the similitude relation. The constant, β, was determined by back calculation using the known exponents required by rotational speed and runner diameter and was found to be 13/10. Thus, the similitude relationship given in equation 4.23 with β = 13/10 becomes

$$\frac{\ln(1-E_1)}{\ln(1-E_2)}=\left[\frac{\phi_1}{\phi_2}\right]\left[\frac{D_1}{D_2}\right]^{1/2}\left[\frac{\nu_2}{\nu_1}\right]^{3/20}\left[\frac{\sigma_2}{\sigma_1}\right]^{3/5}\left[\frac{\rho_1}{\rho_2}\right]^{3/5}\left[\frac{n_1}{n_2}\right]^{17/20}\left[\frac{d_{t1}}{d_{t2}}\right]^{11/10} \qquad (5.1)$$

The value of β was verified by comparing the implied K_L relationship to the entirely analytical approach described by Azbel. The implied K_L relation descibed by equation 4.8 when β = 13/10 is

$$K_L \propto \frac{D^{1/2}U^{13/20}}{L^{7/20}\nu^{3/20}} \qquad (5.2)$$

which differs only slightly in exponents from equation 4.7 as described by Azbel if the minor dependence of K_L upon ϕ is ignored. Equation 4.7 for example, would have a corresponding β value of 3/2 (15/10) which is fairly close to 13/10. However, the model to full-scale similitude relationship is sensitive to the exponents on runner

diameter, scaled up by a factor of 11.7 (for the Norris model) and down by factors of 3.4 and 8 for model rotational speeds of 385 and 900 rpm, respectively.

It is therefore concluded that the empirical fit is within tolerances specified by existing theory for the liquid film coefficient, considering that there are no known experimental data for liquid film coefficient in a highly turbulent bubble flow.

Figures 5.1 and 5.2 show the model data described in section III transformed by the similitude relation, Eq 5.1. The data was scaled from each respective rotational speed to that of the full-scale installation (112.5 rpm) and scaled from the model runner size to that of the full-scale installation (11.71 physical-scale factor). Furthermore the temperature dependent variables such as molecular diffusivity and density were transformed from model test conditions to those recorded during the prototype tests. For visual comparison the prototype operational data is included in the figures. Note that there is good agreement between 385, 900, and 1028 rpm and the prototype operation. As discussed above, certain deviations in operational performance occurring around and above 1100 rpm results in improper scaling of the data. This data has been considered biased and is therefore not valid for verification of the similitude relation.

It should be noted that because the similitude relation is semi-empirical in nature, until there is another set of model-prototype AVTs there can be no true

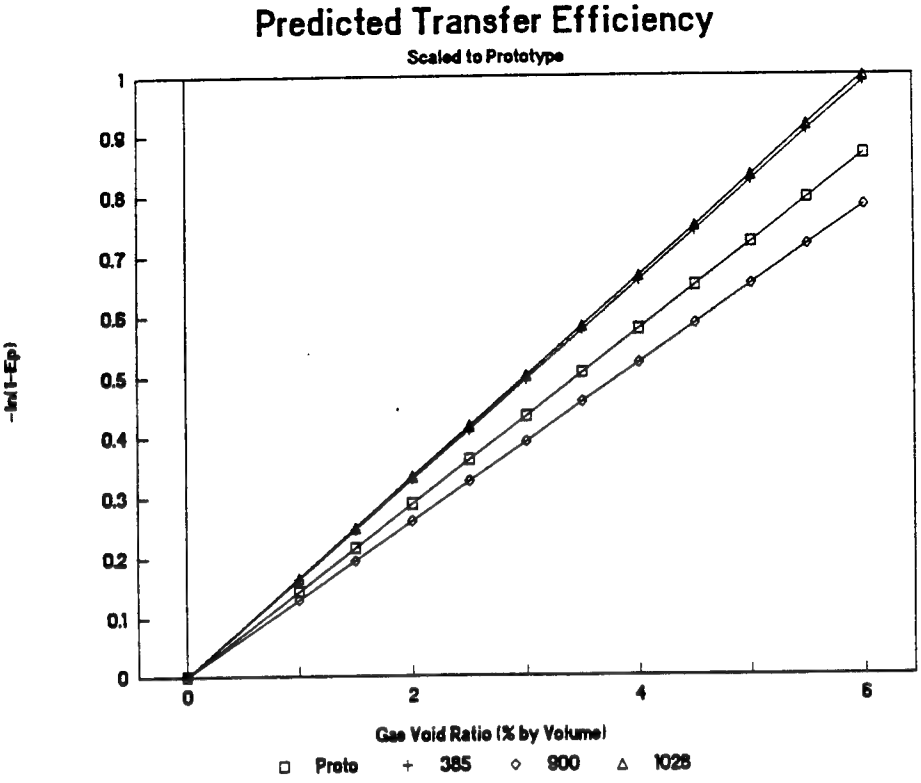

Figure 5.1 Measured Transfer Efficiency scaled to the full-size installation (Ep) by Equation 5.1

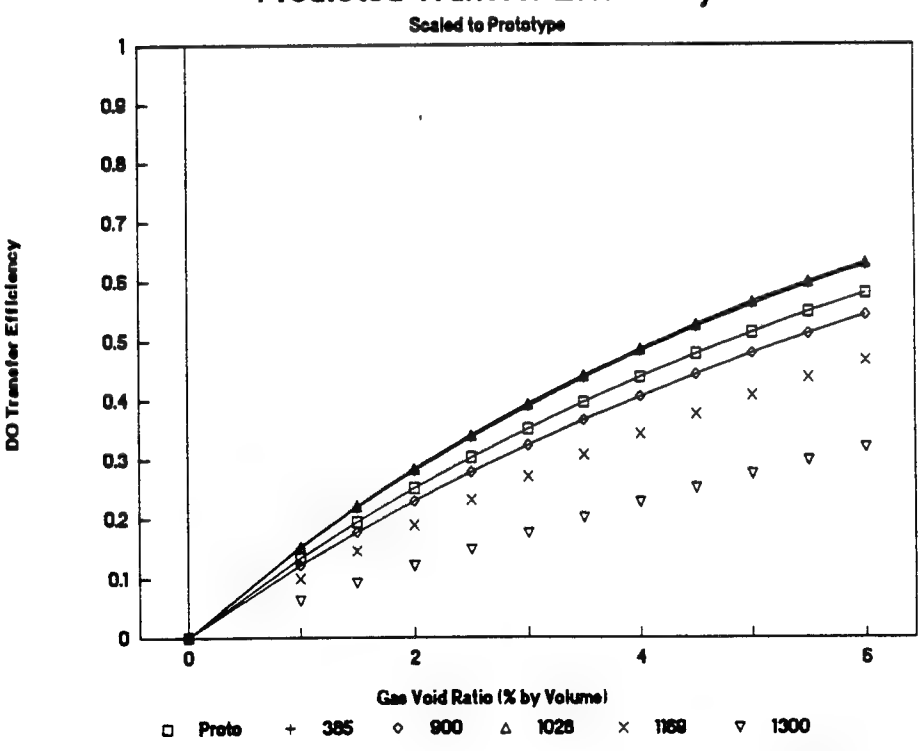

Figure 5.2 Same as Fig. 5.1 : Scaled measurements for rotational speeds of 1169 and 1300 rpm are include for comparison. These were not used in determining the β coefficient.

proof that the relation is valid. Presented here is instead a qualitative explanation of the choice for the empirical coefficient, by comparison with existing theories for the liquid film coefficient.

VI. Admonitions

The similitude relation has been developed and examined with the assumption that the data used is either completely accurate or is uniformly biased in such a way as to not affect scaling requirements. It is therefore necessary to include here a listing and explanation of the potential limitations of the data.

As mentioned previously, the pressure distribution within the draft tube of a full-scale AVT is by no means constant. Figure 6.1 is a longitudinal section view of the Norris draft tube. The change in elevation, relative to the tailwater is substantial. Figure 6.2 gives the static pressure distribution along the centerline of the draft tube, computed by subtracting the velocity head (using the cross-sectional mean velocity) from the hydrostatic pressure. A fairly extensive change in static pressure occurs, beginning subatmospheric and climbing to above atmospheric. The vented air is sheared down to small bubbles shortly after entry into the draft tube which then may coalesce into larger bubbles as the velocity slows down. For this reason it is likely that a high percentage of the oxygen transfer occurs shortly after the air venting. Since the requirements of equation 3.2 incorporate an integral of K_La over the draft tube, and since K_La varies from high to low values along the draft tube length, it is difficult choosing the appropriate value of Cs. A weighted mean Cs (weighted using the integral in Eq 3.2) would probably be the best choice, but this requires a measurement that can separate the Cs effect from the K_L'a't effect in Eq 3.2. This concept will be discussed further in the Conclusions and Recommendations

Figure 6.1 The Norris unit #2 draft tube (from design prints)

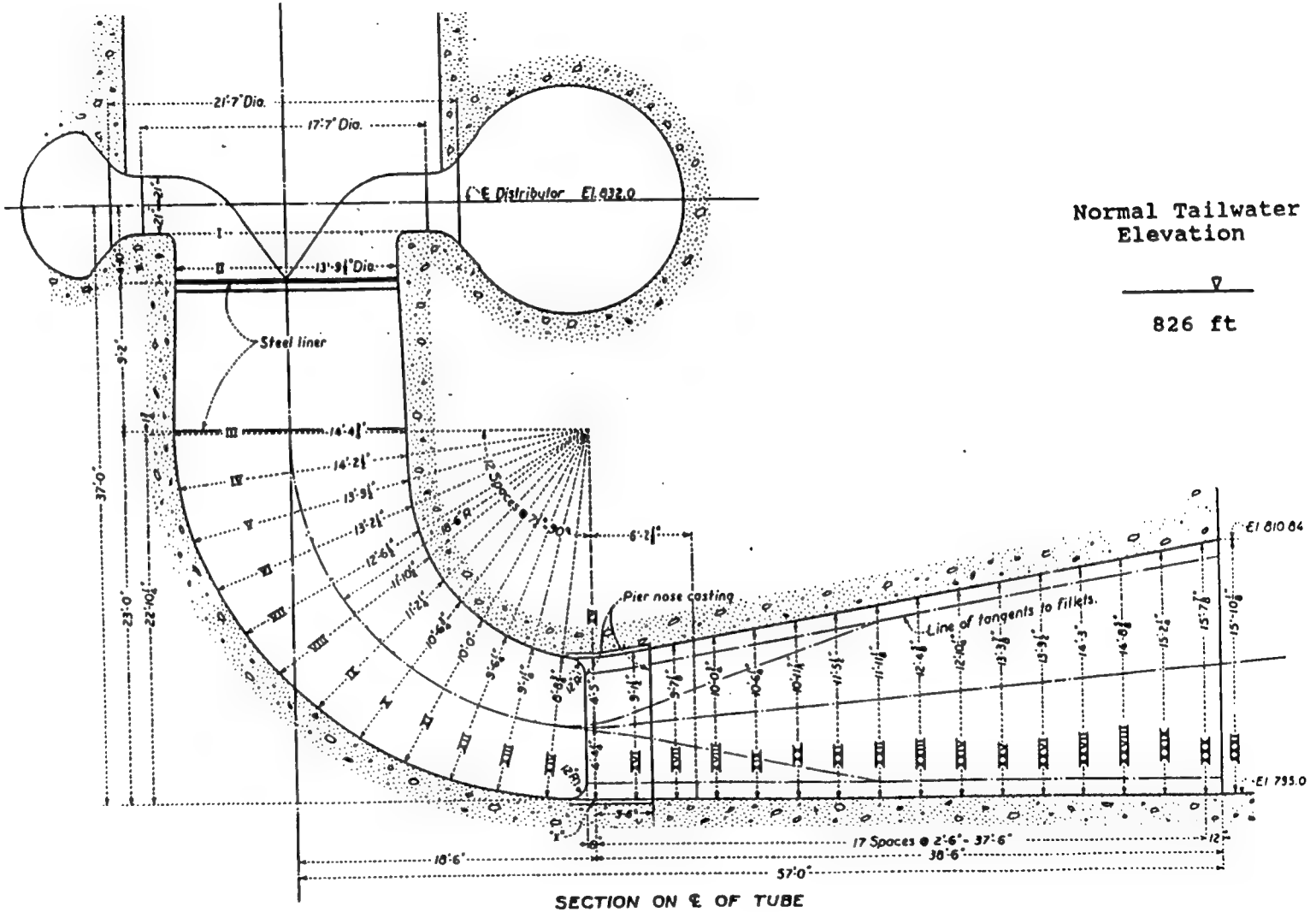

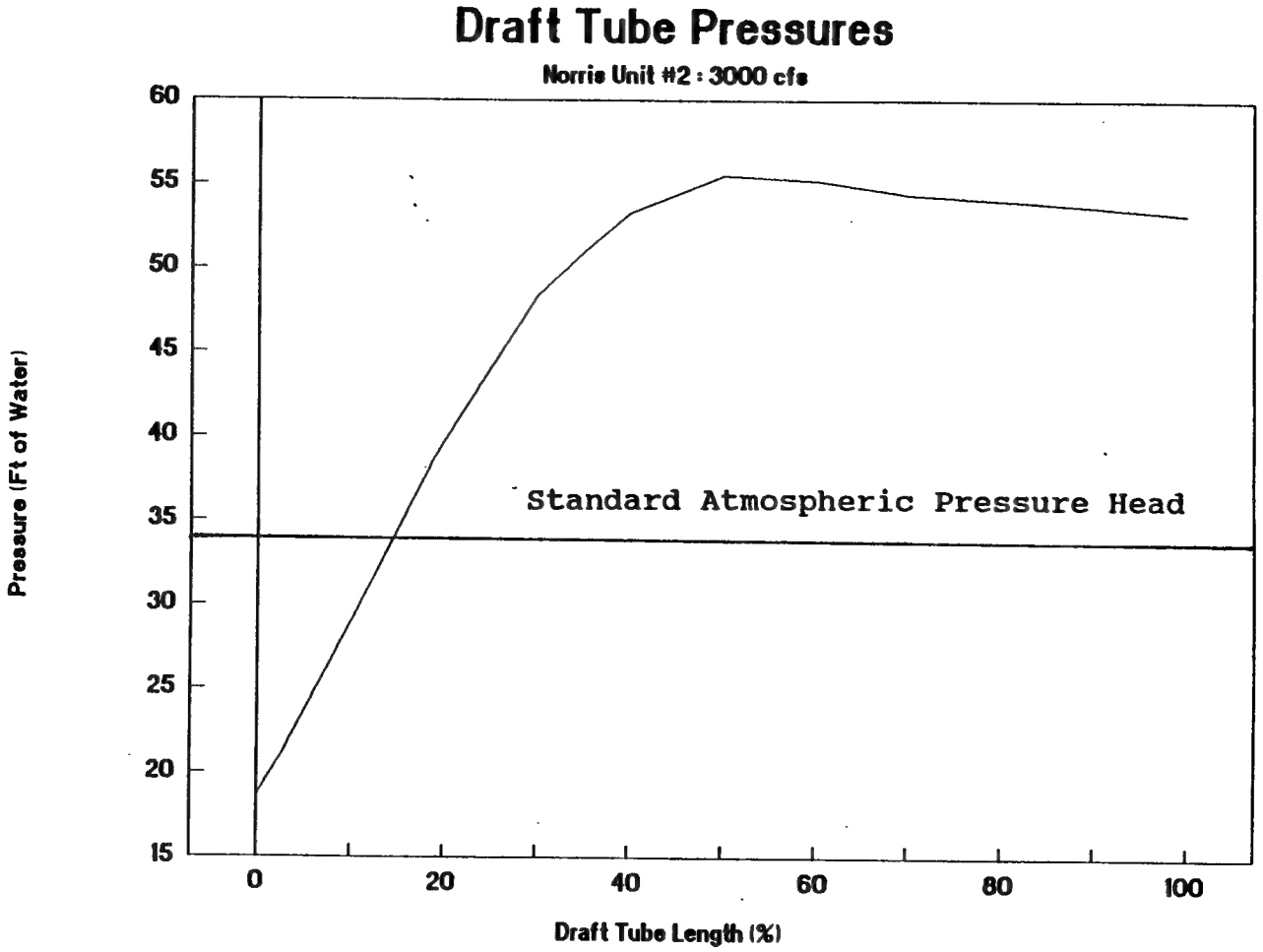

Figure 6.2 Norris Unit #2 draft tube pressure head (absolute). Adapted from Mobley and Brice, 1991.

sections.

Reviewing figure 6.2, and considering the insights into K_L given above, choosing standard atmospheric pressure to compute the Cs value to be used in Eq 3.2 was deemed to be acceptable. The error created by choosing an inappropriate Cs value would result primarily in a change in the slope of the -ln(1-E) vs. ϕ best-fit line to measurements. This is one uncertainty in the application of the similitude relationship to hydroturbine draft tubes where the static pressure vs. distance relation is not similar to that given in figure 6.2.

Also deserving of discussion is the oxygen transfer occurring within the tailrace of the turbine installation. It has been assumed in this thesis that the majority of the oxygen transfer occurring in the AVT system occurs in the highly turbulent vertical section of the draft tube where high shear causes intense bubble splitting and high surface areas for mass transfer. The subsequent coalescence that may occur occur as the flow passes through and out of the draft tube would limit the oxygen transfer in subsequent sections. However, because current sampling techniques do not allow for differentiation between draft tube oxygen transfer and tailwater oxygen transfer, it is impossible to quantify exactly what percentage of oxygen transfer occurs in the draft tube and how much occurs in the tailrace.

When scaling for model similitude, tailwater elevations in the model are

maintained for a number of hydraulic considerations which do not include oxygen transfer. As a result, it is quite probable that a different percentage of oxygen transfer is occurring in the AVT model tailrace as in a similar operation of the full-scale installation. Since the similitude relation is based solely upon turbine operational speed and runner diameter it cannot predict the different effects of tailwater depth. The assumption herein is that the tailrace oxygen transfer is small compared to that which occurs in the draft tube, and can therefore be neglected in the similitude relatioship (Eq 5.1).

VII. Calculation Procedure for the Prediction of Full-Scale Oxygen Transfer from Turbine Model Data

The similitude relation is an extremely simple tool to use. The following example illustrates how the equation was used to scale the Norris model data to the full scale installation in a step by step process using artificial data.

The data shown in table 7.1 represents some artificial data for a hypothetical 13:1 turbine model of a full-scale turbine which operates at 115 rpm. The data shown represents the required measurements for similitude scaling to predict the full-scale turbine aeration performance.

The data shown in table 7.1 can be used to calculate the gas void ratio (ϕ), using equation 4.19, the saturation concentration of oxygen in the tailwater (C_s), using equation 3.6, and the measured oxygen transfer efficiency (Em), using equation 3.3. Plots of ϕ vs -ln(1-Em) and ϕ vs Em are shown in figures 7.1 and 7.2

The physical properties of water and oxygen can be characterized with the water temperatures measured during the tests. Since scaling is performed at constant gas void ratios, ie. $\phi 1 = \phi 2$, the only parameters which need to be defined are: D, ν, σ, ρ, n, and d_i. Table 7.2 lists the values of these coefficients for the model conditions.

The scaling relation is used by inserting all the relative parameters into their respective positions keeping in mind that the subscripts must always remain respective to the model or full-scale unit. An example calculation is given in table 10.3. Scaling has been performed on the model data using the β coefficient of 13/10 as for the Norris model. The results are given in table 10.4 and plotted in figures 7.3 and 7.4

Table 7.1

Model Oxygen Transfer Data and Calculations
as Represented in Figures 10.1 and 10.2

n (rpm)	Air Flow (cfs)	Water Flow (cfs)	ϕ Eq 4.19 (%)	Water Temp (°C)	TW Press (atm)	DO SAT Eq 3.6 (ppm)	DO IN (ppm)	DO OUT (ppm)	Em Eq 4.23
400	0.145	15	0.96	20	0.85	13.87	3.7	3.95	0.024
	0.31	15	2.02	20	0.85	13.87	3.65	4.2	0.054
	0.45	15	2.91	20	0.85	13.87	3.65	4.45	0.078
	0.61	15	3.91	20	0.85	13.87	3.6	4.65	0.102
800	0.29	30	0.96	22.5	0.87	14.61	3.4	3.9	0.045
	0.59	30	1.93	22.5	0.87	14.61	3.4	4.45	0.094
	0.9	30	2.91	22.5	0.87	14.61	3.35	4.95	0.142
	1.25	30	4.00	22.5	0.87	14.61	3.4	5.65	0.201
950	0.356	36	0.98	20	0.86	14.03	3.5	4.05	0.052
	0.71	36	1.93	20	0.86	14.03	3.6	4.70	0.105
	1.18	36	3.17	20	0.86	14.03	3.5	5.4	0.180
	1.44	36	3.85	20	0.86	14.03	3.5	5.85	0.223

Table 7.2

Model/Full-Scale Data for Similitude Scaling

	T (°C)	D (cm^2/s)	ν (m^2/s)	σ (N/m)	ρ (kg/m^3)	d_t (m)
$Model_1$ 400 rpm	20	1.863	1.007	0.073	998.2	0.3
$Model_1$ 800 rpm	22.5	1.988	0.957	0.072	997.7	0.3
$Model_1$ 950 rpm	20	1.863	1.007	0.073	998.2	0.3
$Full_2$ 115 rpm	25	2.130	0.897	0.072	997.1	3.9

Table 7.3

Example Calculation for Predicted Full-Scale Oxygen Transfer Efficiency from the hypothetical model data.

Scaling is performed by inserting the the field data and the physical properties of water and oxygen into the similitude relation

$$\frac{\ln(1-E_1)}{\ln(1-E_2)} = \left[\frac{\phi_1}{\phi_2}\right]\left[\frac{D_1}{D_2}\right]^{1/2}\left[\frac{\nu_2}{\nu_1}\right]^{(\beta-1)/2}\left[\frac{\sigma_2}{\sigma_1}\right]^{3/5}\left[\frac{\rho_1}{\rho_2}\right]^{3/5}\left[\frac{n_1}{n_2}\right]^{(\beta/2+1/5)}\left[\frac{d_{t1}}{d_{t2}}\right]^{(\beta-1/5)} \qquad (10.1)$$

where β = 13/10 for the Norris Turbine.

Below is an example calculation where the similitude equation has been applied to one set of the data expressed in Table 10.1 where n = 400 rpm, ϕ = 0.96, Em = 0.024 (notethat when scaling, ϕ_1/ϕ_2 = 1).

$$\frac{\ln(1-0.024)}{\ln(1-E_2)} = \left[\frac{1.863}{2.130}\right]^{1/2}\left[\frac{0.897}{1.007}\right]^{3/20}\left[\frac{0.072}{0.073}\right]^{3/5}\left[\frac{998.2}{997.1}\right]^{(3/5)}\left[\frac{400}{115}\right]^{17/20}\left[\frac{0.3}{3.9}\right]^{11/10} \qquad (10.2)$$

Simplifying the above relation yields E_2 (Ep) = 0.1321. Complete scaling results are shown in table 10.4 and figure 10.3 and 10.4

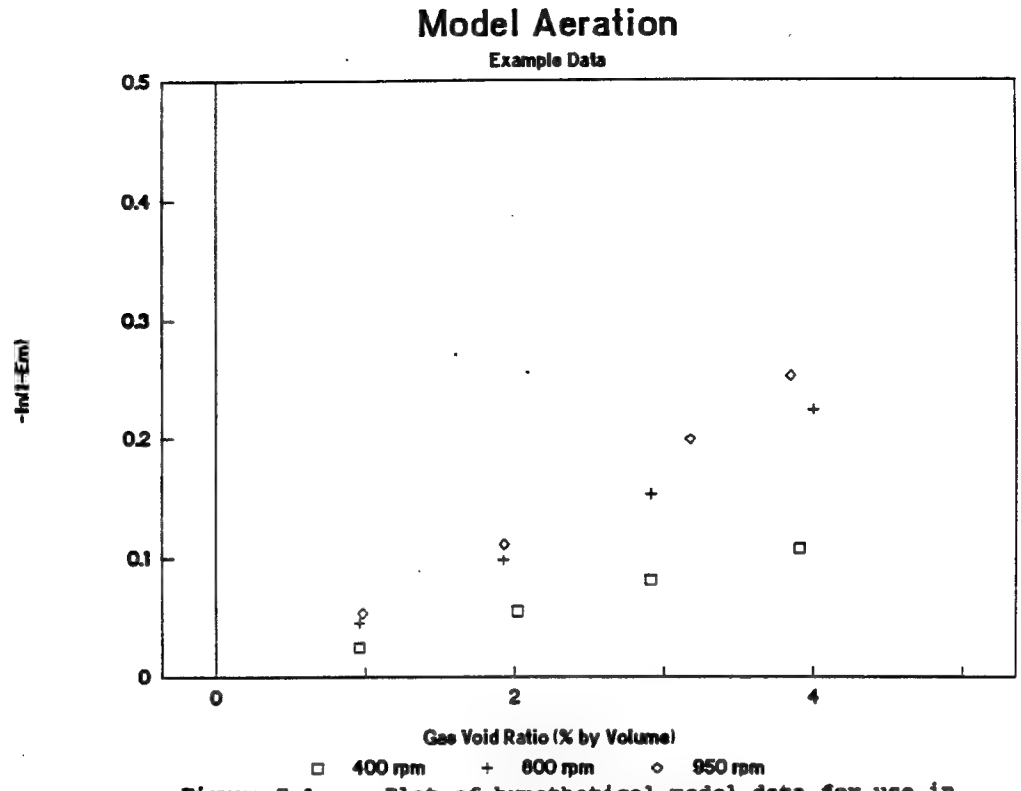

Figure 7.1 Plot of hypothetical model data for use in similitude relationship.

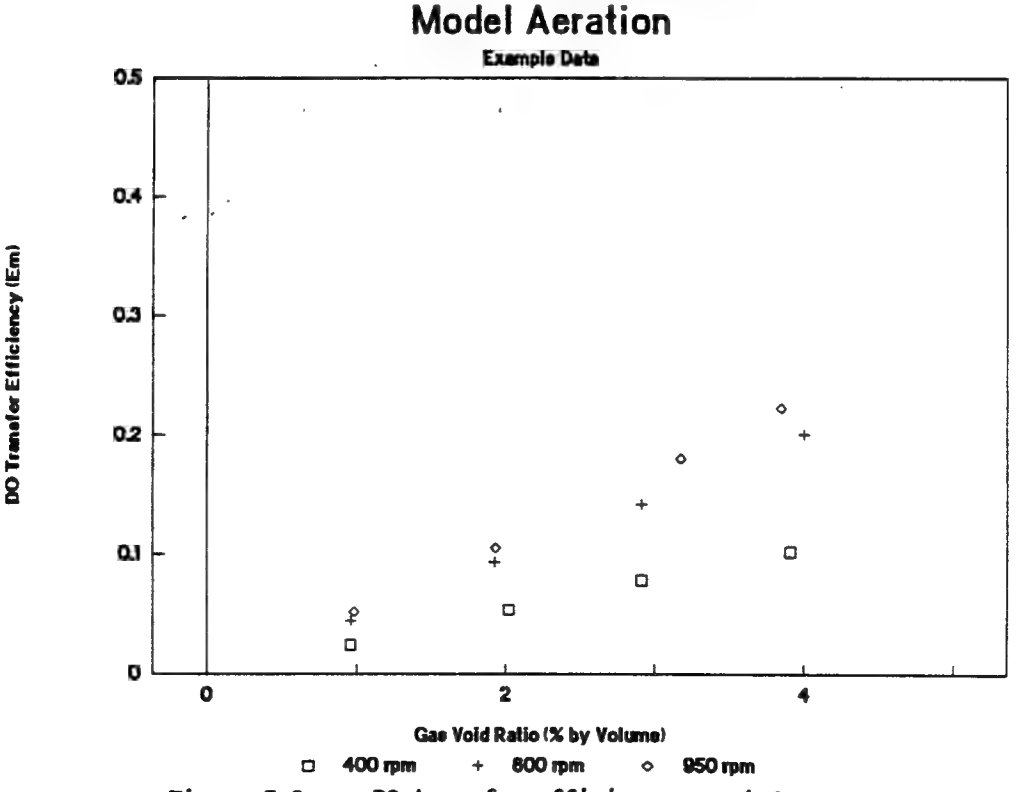

Figure 7.2 DO transfer efficiency vs. ϕ for hypothetical model data.

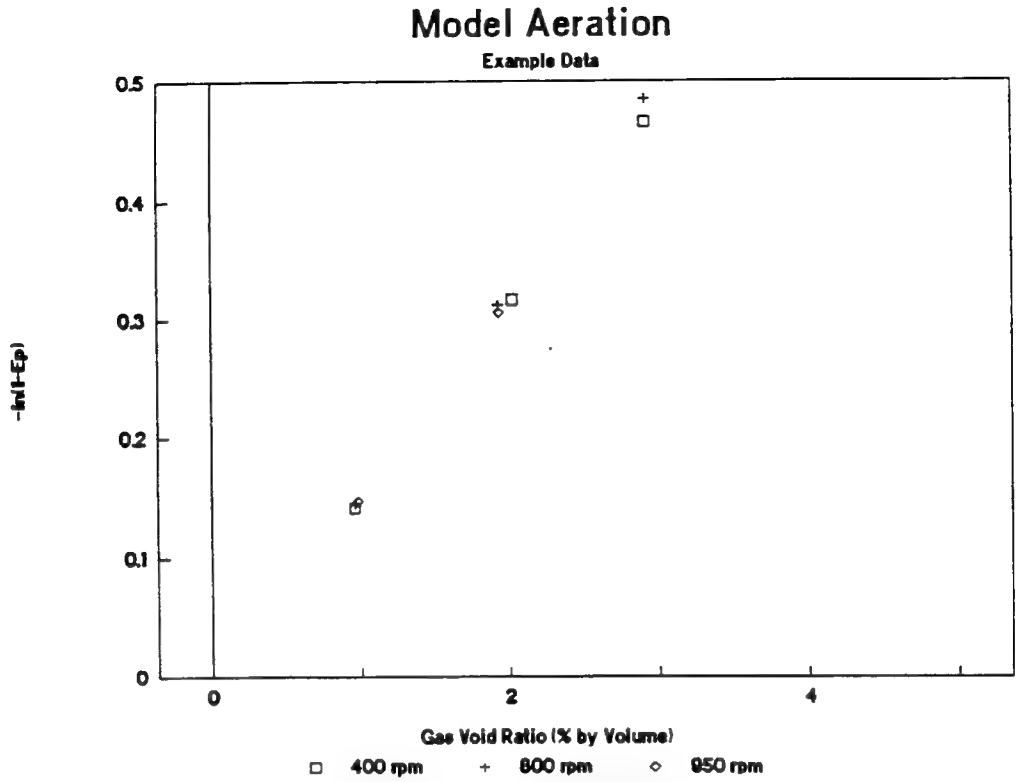

Figure 7.3 Hypothetical model data scaled to full-sized installation as describe in tables 7.3 & 7.4.

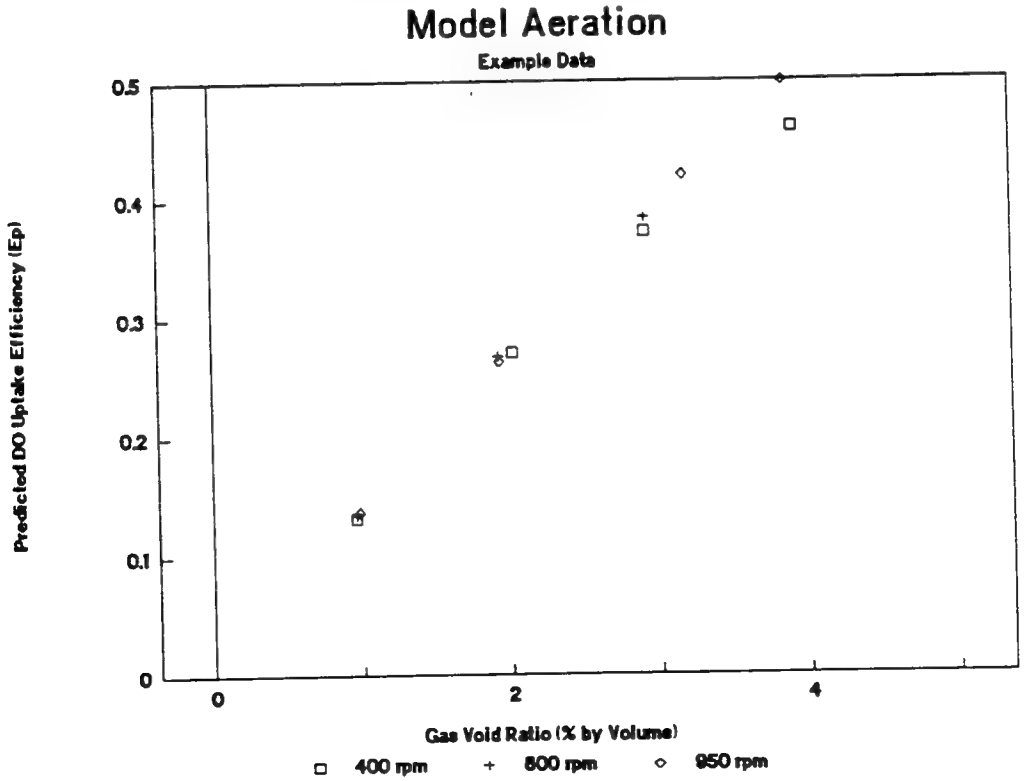

Figure 7.4 Scaled DO transfer efficiency vs. ϕ for hypothetical model data.

Table 7.4

Model Data Scaled to Full-Scale Operation
as Represented in Figures 10.3 and 10.4

n (rpm)	ϕ	Em	-ln(1-Em)	Ep	-ln(1-Ep)
400	0.96	0.024	0.025	0.132	0.142
	2.02	0.054	0.055	0.271	0.316
	2.91	0.078	0.082	0.372	0.466
	3.91	0.102	0.108	0.460	0.617
800	0.96	0.045	0.046	0.135	0.145
	1.93	0.094	0.098	0.268	0.312
	2.91	0.142	0.153	0.384	0.485
	4.00	0.201	0.224	0.508	0.710
950	0.98	0.052	0.054	0.137	0.147
	1.93	0.105	0.111	0.263	0.305
	3.17	0.180	0.199	0.420	0.545
	3.85	0.223	0.252	0.499	0.692

VIII. Conclusions and Recomendations

The similitude relationship has been developed using existing, well established theories to describe conditions within a turbine draft tube with respect to bubble behavior and mass transfer. The similitude theory segments three important parameters which have been developed as proportionalities for scaling purposes; the liquid film coefficient, the specific surface area, and the contact time.

Extensive literature reviews and analytical consideration were given to each of the scaling parameters as well as their overall performance in the mass transfer equation. The theory was developed from conservation of mass between bubbles and a surrounding fluid volume with the assumption that the saturation concentration of oxygen remains constant over the integral boundaries. Integration of the mass conservation equation yielded a term called mass transfer efficiency (oxygen transfer efficiency, E) which was logrithmically dependent upon the three previously mentioned parameters.

The parametric relationship for liquid film coeficient, K_L, was developed using the surface renewal theories developed by Levich (1962) and Azbel (1981). Because neither relation was specifically designed to describe K_L for bubbles in a highly turbulent flow field, both relations were fit with appropriate empirical coefficients resulting in one satisfactory relation describing the liquid film coefficient in the AVT's

turbulent bubble-water environment. It was found that K_L was dependent upon the diffusivity of oxygen in water, the kinematic viscosity of water, and the rotational speed and diameter of the turbine.

The specific surface area term is based upon work done by Hinze (1956) which describes the behavior of bubbles in high shear conditions. The basic relation for bubble size resulting from Hinze's work was combined with the bubble swarm theory of Azbel (1981) to determine a scaling relation for specific surface area dependent upon the gas void fraction, the density and surface tension of the water, and the rotational speed and diameter of the turbine.

A relationship describing a scaling criterion for bubble- water contact time was developed from current turbine similitude theory. It was determined that contact time is dependent only upon turbine rotational speed.

The similitude relation is the result of the insertion and simplification of the proportionalities described above into the mass transfer equation. Because there were many parameters common to each of the proportionalities, the similitude equation simplified into a very simple mathematical relation.

The similitude relation can be used to scale model performance data to a full-scale installation at the same gas void ratio by inserting the known operational

performance and geometric characteristics of the turbine model and the known properties of water and oxygen for the turbine test conditions. Results for many different full-scale operational settings can be determined by inserting respective terms for the full-scale operation.

For the Norris model/full-scale data, good comparisons have been shown using the model and the full-scale data within the limits of the model operation as describe above. However, as stated previously, without another model-prototype AVT correlation the similitude relation cannot truly be verified. The familiar similitude theory for the prediction of full-scale efficiency and cavitation from model tests were not developed from one model/full-scale comparison. We should, therefore, see the similitude relationship for oxygen transfer, developed from the Norris model/full-scale comparison with some parametric relationships from the literature, as a first approximation, not as a final answer. Further model/full-scale comparisons may indicate that the exponents or the Cs computation need to be altered, or that the correct parameterization of the tailwater oxygen transfer is required. It is however, believed that these adjustments will be fairly minor and the theory described herein should be nearly universally applicable.

Recommendations

Two significant limitations to the similitude relation are the inability to predict the effective saturation concentration of the gas in the water in the draft tube of the

prototype and the inability to determine the size and behavior of the bubbles in the turbulent vertical section of the model draft tube.

The latter problem might be solved by use of high speed photography and laser-doppler measurements of velocity, and hence shear, in the vertical section of the model draft tube. The TVA and the Bureau of Reclamation have undertaken this task on a model of the Grand Coulee turbine and have performed some tests at Colorado State University. Solving the former problem will be more difficult however, due to physical limitations because of model size and construction.

In the past some field tests have been performed using a tracer gas to estimate the gas transfer of a chemical compound other than oxygen. One application of a field test using a tracer gas is the injection of Sulfur-Hexafluoride (SF_6) into air intakes of auto-venting turbines. Since SF_6 is not native to the environment, upstream concentrations are zero. Downstream concentrations can be determined by analyzing water samples, gathered similarily to oxygen samples, using a gas chromatagraph. Tests like this allow for quantification of the impacts of upstream reservoir stratification and downstream baseline transfer due to turbulence at the tailwater boil. (Wilhelms, 1993)

Another tracer gas experiment where a slug of water containing SF_6 is added to a reservoir and samples are taken to determine the rate at which gas leaves the

liquid phase can be coupled with the aforementioned test to determine the effective saturation concentration. The SF_6 transfer, in this case, will have virtually no saturation concentration, and comparison of the two tracer tests can be used to determine an equivalent (or effective) saturation concentration. For this type of tracer study, the dilution of the water phase SF_6 must also be quantified, requiring the simultaneous release of a conservative tracer such as rhodamine-WT.

If a continuous stream of water containing a known concentration of SF_6 was released just upstream of the hydroelectric intake, a reverse transfer test could be performed on the AVT. As air was aspirated into the turbine draft tube, SF_6 would transfer out of the liquid phase and into the air bubbles. Because there is no measureable quantity of SF_6 in the atmosphere, the concentration in the air bubbles would be very close to zero. Therefore regardless of the pressure changes the bubbles experience throughout their trip through the draft tube, no significant change in concentration of SF_6 in the bubble will occur.

Upstream samples may be taken in the draft tube as was performed with oxygen, downstream samples can be gathered from a boat as described earlier, and saturation values can be determined from Henry's law and air and water flow measurements. From these measurements, SF_6 transfer efficiency can be determined. Comparing the transfer efficiency of SF_6 betwwen the two tracer gas tests will reveal an equivalent (or effective) saturation concentration for the draft tube. Knowing the

behavior of the gas as described by Henry's law will allow determination of the effective average pressure occuring in the draft tube.

References

Amberg, H. R., D. W. Wise, and T. R. Aspitarle (1969) "Aeration of Streams with Air and Molecular Oxygen." Presented at the Sixth Water and Air Conference of Technical Association of Pulp and Paper Industry, Jacksonville, Florida.

Arndt, Roger E. A. and John S. Gulliver (1989) Hydropower Research and Development in Minnesota, Tech. Paper 259, St. Anthony Falls Hydraulics Laboratory, Minneapolis, MN

Azbel, D. (1981), Two Phase Flows in Chemical Engineering, Cambridge University Press, Chapts. 3 and 7.

Bohac, Charles E., James W. Boyd, E. Dean Harshbarger, and Alicia R. Lewis (1983) Techniques for Reaeration of Hydropower Releases, Tech. Report E-83-5 prepared by Tennessee Valley Authority for the U.S. Army Corps of Engineer Waterways Experiment Station, Vicksburg Mississippi.

Bohac, Charles E. and Richard J. Ruane (1990), "Solving the Dissolved Oxygen Problem," Hydro Review, (9)1, pp 62-72.

Bohac, Charles E. and Richard J. Raune (1992), "Tailwater concerns and the History of Auto-Venting Hydroturbines," Progress in Autoventing Turbine Development, Tennessee Valley Authority Engineering Laboratory, Norris, TN.

Cybarluz, Joseph M., T. A. Brice, and Tai T. Do (1991) Model Test Report for Norris Dam Aeration, Prepared by Voith Hydro for the Tennessee Valley Authority, Chatanooga, TN.

Gulliver, J. S., J. R. Thene and A. J. Rindels (1990), "Indexing Gas Transfer in Self-Aerated Flows," Journal of Environmental Engineering, 116(3).

Harshbarger, Dean E. (1983), Forced Air Turbine Venting Studies January through December,1982, Tennessee Valley Authority Office of Natural Resources and Economic Development, Division of Air and Water Resources, Water Systems Development Branch, Norris, TN.

Harshbarger, Dean E. (1984), Streamlined Hub Baffles for Aeration at Norris Dam, Tennessee Valley Authority Engineering Laboratory, Norris, TN.

Hinze, J. O. (1955), "Fundamentals of the Hydrodynamic Mechanism of Splitting in Dispersion Proceses," American Institute of Chemical Engineering Journal 1(3) pp. 289 - 295.

Hua, Hesong (1990) "Accurate Method for Calculation of Saturation DO," Journal of Environmental Engineering Vol. 116, No. 5, Sept. - Oct, 1990.

Killen, J. M. (1982), "Maximum Stable Bubble Size and Associated Noise Spectra in a Turbulent Boundary Layer," Cavitation and Polyphase Flow Forum, ASME, pp 1-3 New York, New York.

March, P. A. and W. A. Waldrop (1990), "Technology Development for Auto-Venting Turbines," Air-Water Mass Transfer, ASCE, pp 506-511 New York, NY.

March, P. A., T. A. Brice, M. H. Mobley, and J. L. Cybularz, Jr. (1992), Status and potential of Auto-Venting Hydroturbines, Tennessee Valley Authority Engineering Laboratory, Norris, TN.

March, P. A., T. A. Brice, M. H. Mobley, and J. L. Cybularz, Jr. (1992) "Turbines for solving the D.O. Dilemma," Hydro Review, 11(1) pp. 30-36.

March, P. A., J. L. Cybularz, and Billy G. Ragsdale (1992), "Model Tests for the Evaluation of Auto-Venting Hydroturbines," Progress in Autoventing Turbine Development, Tennessee Valley Authority Engineering Laboratory, Norris, TN.

Maudlin G. V. (1982) "Turbine Venting at Clarks Hill Dam, " Proceedings of a Seminar on Attaining Water Quality Goals Through Water Management Procedures, Hydrologic Engineering Center, Davis, California.

Miller, David E. (1983) "Static Deflectors Boost Aeration, Increase Dissolved Oxygen," Power, January, 1983 pg. 130.

Mobley, M. and T. Brice (1991), "Experimental Difficulties Encountered in Testing Air/Water Mixtures," Hydraulic Engineering, Proceedings of the 1991 National Conference on Hydraulic Engineering, ASCE, New York.

aney, Donald C. and Terry G. Arnold (1973) "Dissolved Oxygen Improvement by Hydroelectric Turbine Aspiration," Journal of the Power Division, ASCE (99) PO1.

Raney, Donald C. "Turbine Aspiration for Oxygen Supplementation," (1977) Journal of the Power Division, ASCE (103) EE2.

Sevik, M. and S. H. Park (1973), "The Splitting of Drops and Bubbles by Turbulent Fluid Flow," Joural of Fluids Engineering, 95(1), pp. 53-60.

Sheppard, Andrew R., David E. Miller, and Clifton L. Buck (1981) "Prediction of Oxygen Uptake in Hydroelectric Draft Tube Aeration Systems," Proceedings of the 1981 Environmental Engineering Division, ASCE, New York.

Sheppard, Andrew R. and David E. Miller (1982) "Dissolved Oxygen in Hydro Plant Discharge Increased by Aeration," Power Engineering Vol 86, October, pp. 62-65.

Waldrop, William R. (1992), "Overview of Autoventing Turbine Technology Development Project," Progress in Auto-Venting Turbine Development, Tennessee Valley Authority Engineering Laboratory, Norris, TN.

Weithman, A. S., J. R. Whithley, and M. A. Haas (1980) "Table Rock Tailwater Trout Fishery-Value, Use, and Dissolved Oxygen Problem, " reprinted from a seminar on Water Quality Evaluation, U. S. Army Corps of Engineers, Vicksburg, Miss.

Wilhelms, Steven C., M. L. Schneider, and Stacy E. Howington (1987) Improvement of Hydropower Release Dissolved Oxygen with Turbine Venting, U.S. Army Engineer Waterways Experiment Station, Vicksburg, MISS.

Wilhelms, Steven C (1993) Turbine Venting at Bull Shoals and Norfork Dams, Arkansas, Draft report to U.S. Army Engineer Waterways Experiment Station, Vicksburg, MISS.

Appendix A. Norris Unit 2 Aeration Test Data

Date	Air Flow (scfs)	Water Flow (cfs)	Water Temp. (C)	DO Sat. (mg/l)	Scroll Case DO (mg/l)	Tail Race DO (mg/l)	DO Transfer Em	Gas Void Ratio (%)
6-9-92	0.000	3875	8.1	11.404	8.2	8.2	0.000	0.000
	0.000	3875	8.1	11.404	8.2	8.2	0.000	0.000
	0.000	3875	8.1	11.404	8.2	8.2	0.000	0.000
	0.000	3875	8.1	11.404	8.2	8.2	0.000	0.000
	0.000	3875	8.1	11.404	8.2	8.2	0.000	0.000
	0.000	3875	8.1	11.404	8.2	8.2	0.000	0.000
	89.966	3875	8.1	11.404	8.2	9.5	0.406	2.269
	89.966	3875	8.1	11.404	8.2	9.7	0.468	2.269
	89.966	3875	8.1	11.404	8.2	9.7	0.468	2.269
	89.966	3875	8.1	11.404	8.2	9.7	0.468	2.269
	89.966	3875	8.1	11.404	8.2	9.7	0.468	2.269
	89.966	3875	8.1	11.404	8.2	9.7	0.468	2.269
	89.966	3875	8.1	11.404	8.2	9.1	0.281	2.269
	24.849	3875	8.1	11.404	8.2	8.8	0.187	0.637
	24.849	3875	8.1	11.404	8.2	8.7	0.156	0.637
	24.849	3875	8.1	11.404	8.2	8.7	0.156	0.637
	24.849	3875	8.1	11.404	8.2	8.7	0.156	0.637
	24.849	3875	8.1	11.404	8.2	8.7	0.156	0.637
	24.849	3875	8.1	11.404	8.2	8.7	0.156	0.637
	24.849	3875	8.1	11.404	8.2	9.2	0.312	0.637
	57.557	3875	8.1	11.404	8.2	9.2	0.312	1.464
	57.557	3875	8.1	11.404	8.2	9.2	0.312	1.464
	57.557	3875	8.1	11.404	8.2	9.2	0.312	1.464
	0.000	3875	8.1	11.404	8.2	8.3	0.000	0.000
	0.000	3875	8.1	11.404	8.2	8.2	0.000	0.000
	0.000	3875	8.1	11.404	8.2	8.1	0.000	0.000
10-10-82	81.260	1305	18	9.061	0.3	5.9	0.639	5.862
	103.610	1846	18	9.061	0.3	4.8	0.514	5.314
	92.150	2387	18	9.061	0.3	4	0.422	3.717
	116.030	3301	18	9.061	0.3	3.4	0.354	3.396
	144.440	4125	18	9.061	0.3	3.2	0.331	3.383
	126.170	3664	18	9.061	0.3	3.6	0.377	3.329
	140.190	4078	18	9.061	0.3	3.3	0.342	3.323
	105.200	3094	18	9.061	0.3	3.1	0.320	3.288
	134.070	3951	18	9.061	0.3	3.3	0.342	3.282
	89.670	2842	18	9.061	0.3	3.3	0.342	3.059
	79.830	3066	18	9.061	0.3	3.1	0.320	2.538
	71.670	3061	18	9.061	0.3	3.2	0.331	2.288
	63.940	3065	18	9.061	0.3	3	0.308	2.044
	46.950	3077	18	9.061	0.3	2.3	0.228	1.503
	30.660	3075	18	9.061	0.3	2.2	0.217	0.987
	15.790	3094	18	9.061	0.3	1.3	0.114	0.508
	0.000	3094	18	9.061	0.3	0.3	0.000	0.000
6-29-83	71.200	1522	10	10.878	6.6	7.9	0.304	4.469
	76.500	2108	10	10.878	6.6	8	0.327	3.502
	133.910	4632	10	10.878	6.6	8.3	0.397	2.810
	123.890	4488	10	10.878	6.6	8.2	0.374	2.686
	119.120	4342	10	10.878	6.6	8.2	0.374	2.670

70.680	2653	10	10.878	6.6	7.6	0.234	2.595
108.250	4185	10	10.878	6.6	8	0.327	2.521
87.330	3649	10	10.878	6.6	7.5	0.210	2.337
75.970	3184	10	10.878	6.6	7.5	0.210	2.330
80.660	3416	10	10.878	6.6	7.8	0.281	2.307
93.520	3991	10	10.878	6.6	7.9	0.304	2.290
84.720	3818	10	10.878	6.6	7.8	0.281	2.171

Appendix B. TVA Model Test Index

The model data represented in this thesis was generously donated by the Tennessee Valley

Authority. While the data is refered to in the text by rotational speed, TVA has identified the test data by an alphanumeric code system which is represented here.

Rotational Speed	TVA Test Number	
385 rpm	LB	6734
	LC	6734
	LD	6734
	LE	6734
	LF	6734
	LG	6734
	LI	6734
	LJ	6734
900 rpm	LE	6734
1028 rpm	LL	6734
1100 rpm	LL	6734
1133 rpm	LL	6734
1148 rpm	LL	6734
1170 rpm	LL	6734
1300 rpm	LL	6734

Appendix C
List of Symbols

a = Specific surface area

A = Surface area of bubbles

A_{cs} = Cross-sectional area of the turbine runner

C = Mean concentration of dissolved oxygen in the water

C_a = Concentration of oxygen in the bubbles

C_s = Saturation concentration at equilibrium

d_b = Volumetric mean bubble diameter

d_m = Bubble diameter than encompasses 95% of the air by volume

d_t = Diameter of the turbine runner

D = Diffusivity of oxygen in water

E = Oxygen transfer efficiency

H = Henry's Law constant

k = Constant of proportionality

K_L = Liquid film coefficient for bubble-water oxygen transfer

L = Integral eddy length scale

m = Mass of oxygen in the bubbles

n = Turbine rotational speed

q = Hyperbolic mean unsteady velocity

Q = Volumetric discharge

r = Renewal rate

t = Time

u^* = Shear velocity

u' = Unsteady portion of x direction velocity

U = Characteristic velocity of large eddies

v' = Unsteady portion of y direction velocity

V = Volume

V_r = Velocity of a bubble relative to its liquid surroundings

w' = Unsteady portion of z direction velocity

β = Empirical coefficient

ε = Rate of turbulent kinetic energy dissipation per unit mass

ν = Kinematic viscosity of water

ρ = Density of water

σ = Surface tension of water

ϕ = Gas void fraction

REPORT DOCUMENTATION PAGE

Form Approved
OMB No. 0704-0188

1. AGENCY USE ONLY *(Leave blank)*	2. REPORT DATE	3. REPORT TYPE AND DATES COVERED
	December 1994	Final report

4. TITLE AND SUBTITLE
Oxygen Transfer Similitude for a Vented Hydroturbine

5. FUNDING NUMBERS

6. AUTHOR(S)
Eric J. Thompson

7. PERFORMING ORGANIZATION NAME(S) AND ADDRESS(ES)
St. Anthony Falls Hydraulic Laboratory, Department of Civil and Mineral Engineering, University of Minnesota, Minneapolis, MN 55414

8. PERFORMING ORGANIZATION REPORT NUMBER

9. SPONSORING/MONITORING AGENCY NAME(S) AND ADDRESS(ES)
U.S. Army Corps of Engineers, Washington, DC 20314-1000
U.S. Army Engineer Waterways Experiment Station, 3909 Halls Ferry Road, Vicksburg, MS 39180-6199

10. SPONSORING/MONITORING AGENCY REPORT NUMBER
Miscellaneous Paper W-94-1

11. SUPPLEMENTARY NOTES
Available from National Technical Information Service, 5285 Port Royal Road, Springfield, VA 22161.

12a. DISTRIBUTION/AVAILABILITY STATEMENT
Approved for public release; distribution is unlimited.

12b. DISTRIBUTION CODE

13. ABSTRACT *(Maximum 200 words)*

Discharge from large impoundments of water, such as those found behind hydroelectric installations, can have major impacts on downstream water quality. Discharges from surface layers over spillways can significantly improve dissolved oxygen (DO) levels in tailwaters. Conversely, discharges from lower hypolimnetic regions in a reservoir can release anoxic waters whose low DO can result in large-scale environmental damage. A new technology has been developed called the autoventing turbine that aspirates air into hydroelectric turbine discharges in order to substantially improve release DO when it is needed.

There is a great deal of research involved in determining the limits of effectiveness of oxygen transfer through auto-venting turbines, and improving the performance of early prototypes. Many preliminary investigations at several different locations failed to reveal a single best design for the auto-venting turbine. As a result current research efforts have gone toward designing and testing of turbine models and evaluation of the effectiveness of model runner configurations.

(Continued)

14. SUBJECT TERMS
Hydroturbine
Oxygen transfer
Modeling
Similitude

15. NUMBER OF PAGES
83

16. PRICE CODE

17. SECURITY CLASSIFICATION OF REPORT	18. SECURITY CLASSIFICATION OF THIS PAGE	19. SECURITY CLASSIFICATION OF ABSTRACT	20. LIMITATION OF ABSTRACT
UNCLASSIFIED	UNCLASSIFIED		

13. (Concluded).

This thesis develops a similitude relationship for gas transfer in an auto-venting turbine with specific reference to scaling between a homologous turbine model and full size installation. The relation has been developed from oxygen transfer data and physically realistic theories and contains a single empirical coefficient to account for the current lack of knowledge on gas transfer from bubbles to a turbulent flowing liquid. The final result is a similitude equation which satisfactorily predicts gas transfer efficiency in a full-scale prototype from known model behavior. The relationship, however, should be tested on future auto-venting turbine models to verify that it is scaling oxygen transfer properly.